Understanding the Formation of Al_{13} and Al_{30} Polycations to the Development of Microporous Materials based on Al_{13}-and Al_{30}-PILC Montmorillonites: A Review

Yaneth Cardona, Sophia A. Korili, Antonio Gil *

INAMAT^2,-Departamento de Ciencias, Edificio de los Acebos, Universidad Pública de Navarra, 31006 Pamplona, Spain

ABSTRACT

Hydrolysis of aluminum cations (Al^{3+}), the third most abundant metal in the Earth's crust, is considered relevant in many academic fields, including materials science and chemical engineering. Al^{III} -polycations and their different uses have also been widely studied, as reflected in the extensive literature in that field. This review summarizes some of those studies, from Al^{3+} hydrolysis to form Al_{13} ($[Al_{13}O_4(OH)_{24}(H_2O)_{12}]^{7+}$) and Al_{30} ($[(Al_{30}O_8(OH)_{56}(H_2O)_{24})]^{18+}$) polycations and their specific use as pillaring agents for montmorillonite, which is the most commonly used clay mineral in Aluminum Pillared Interlayered Clays (Al-PILC) synthesis. The experimental conditions published over the years regarding the synthesis of both these Al^{III}-polycations, as well as the conditions employed to synthesize Al-PILC montmorillonite using Al_{13} and Al_{30} polycation solutions, are also summarized. This review highlights some of the findings that have made it possible to explain the formation of Al_{13}- and Al_{30}-PILC montmorillonites, and allow us to clearly understand their differences. Finally, the new tendencies in the development of these materials based on Al-PILC and the applications are also highlighted.

Keywords: Aluminum Pillared Interlayered Clays (Al-PILC), Aluminum pillared montmorillonites, Hydrolysis of aluminum, Polynuclear species, Aluminum polycations, Al_{13} polycation, Al_{30} polycation, hydroxo polymers, Keggin-type species.

* Corresponding author, E-mail address: andoni@unavarra.es (A. Gil)

1. Introduction

Clay minerals are ubiquitous components in soils and sediments that play an important role in several geological and biological events and dominate numerous environmental and geochemical processes (Wen et al., 2019b). The majority of clays are made of stacked tetrahedral and octahedral layers, the arrangement of which allows three main types of clay to be identified. One of these is the smectite group (2:1), also known as the TOT type because these clays contain one octahedral sheet of alumina (O) between two tetrahedral sheets of silica (T); montmorillonite is one example of smectite (**Figure 1**). These TOT clays have a permanent negative surface charge due to isomorphous substitution, (such as, e.g., Al^{III} by Si^{IV} in the T-layer and/or Al^{III} by Mg^{II} in the O-layer), which is compensated by the presence of cations (such as Na^{+} or Ca^{2+}), known as “exchangeable cations”, “interlayer cations”, or “compensator cations”, in the interlayer space (Jlassi et al., 2017; Lazaratou et al., 2020; Motalov et al., 2017; Wen et al., 2019b).

Smectites expand when hydrated, but when heated and dehydrated, their layers collapse, thus making the interlayer surface inaccessible for chemical process applications. To solve this problem, researchers have distanced the clay layers, thereby augmenting the pore volume and allowing clays to maintain their porosity during the hydration and dehydration processes (**Figure 2a**). To achieve that, several studies have proposed the introduction of stable pillars in the interlayer region, thus converting the clay into a pillared interlayered clay (PILC) (Cool and Vansant, 1998). These pillars are introduced into the interlayered space using two main steps (**Figure 2b**): an intercalation process consisting of switching the “exchangeable cations” for a larger and bulkier polymeric inorganic cation, via a cation-exchange reaction, or a calcination step, which involves converting the intercalated polycation precursors into rigid metal oxide clusters, or pillars, (e.g. Al_2O_3, TiO_2, Fe_2O_3, etc.) by dehydration and dehydroxylation. The resulting materials, in which pillars are strongly bonded to the clay layers, retain the layered structure of clays without collapsing and have a higher basal spacing, pore volume, and surface area (Cool and Vansant, 1998; Gil et al., 2000a; Nunes et al., 2008;

Osorio-Revilla et al., 2006; Vicente et al., 2013; Yuan et al., 2006; Zhu et al., 2018). The size and shape of two-dimensional porous PILC depend on many factors, including the nature and layer charge of the layered hosts, the pillaring materials used, their valence/charge, the pillaring steps, and the reaction conditions (Gil et al., 2000a; Gil et al., 2007; Zhu et al., 2017; Zuo et al., 2012).

The properties of PILC make these solids suitable for applications in several fields, especially for adsorption and catalysis purposes (Cool and Vansant, 1998; Gil et al., 2011a; Wen et al., 2019a). Clay minerals, whether natural or modified, are considered interesting materials because of their environmentally-friendly features, their abundance, and low cost; of these, montmorillonite has been widely used as a host, due to its structural and physicochemical properties, especially its swelling capacity, high internal surface area, and high cation-exchange capacity (Zhu et al., 2018). Inorganic cations with large particle sizes have been used as pillaring agents, with the most common being the cations of following elements Al, Fe, Zr, Cr, and Ti. However, over the years, other cations, including those of Ni, V, Zn, Ga, Co, Cu, Ta, have also been used, as have Al^{III}-containing composites, such as Al/Fe and Al/Co, amongst others, and even mixed oxides supported as Fe-Mo, Cu-Ce, among others (Cañizares et al., 1999; Galeano et al., 2014; Gil et al., 2000a; Muñoz et al., 2017; Wen et al., 2019a; Zhu et al., 2017).

However, among the large family of polycations, aluminum Keggin ions as pillars, with montmorillonite as the host clay, have been the most common pillared clays studied, in part due to their permanent porosity and higher accessible surface area, which allows their potential application as an adsorbent for contaminants and their use in heterogeneous catalysis. Al-pillared smectites have been widely documented in the past few decades (Vicente et al., 2013; Wen et al., 2019a; Zhu et al., 2018). As such, this review provides an overview of studies related to the formation of Al-PILC using Al_{13} and Al_{30} as an intercalating solution. To understand this process over the years, the review starts with some initial studies on aluminum hydrolysis from 1952, then explains the formation of Al_{13} and Al_{30} polycations, and,

finally, the formation of Al-PILC. The second part of this review shows how researchers have proposed several conditions in these processes to achieve a successful synthesis of PILC using Al_{13} and Al_{30}, and we conclude with a section concerning future challenges in this field.

2. Aluminum hydrolysis

Aluminum hydrolysis is considered relevant in many academic fields. In general terms, hydrolysis reactions are considered important in chemistry because they determine the behavior of the species formed, including their interactions with other complexing ligands or with solids (Mesmer and Baes, 1990). The splitting of water molecules results in the release of protons, and the reaction of metal ions with the products of this water splitting results in the formation of hydroxy or oxy complexes in solution. Polynuclear species, such as $[M_X(OH)_Y]^{(XZ-Y)+}$, are often formed; the solution contains more than one cation and many ions that are hydrolyzed. This can happen in the presence of several mononuclear species of the type $[M_X(OH)_Y]^{(XZ-Y)+}$, and those with symmetrical constitutions appear to be the most common. Many of the analytical characterization techniques that have been developed are used to study these species (Abeysinghe et al., 2013b; Zhu et al., 2017).

Metal ions form mononuclear species upon hydrolysis in dilute solutions ($< 10^{-4}$ mol/dm^3) which implies the fast removal of a proton from a hydrating water molecule (Mesmer and Baes, 1990). The aqueous chemistry of aluminum is complex; it hydrolyzes in water to produce a wide variety of solute molecules and solids, such as aluminum oxy-hydroxide clusters, and aluminum hydroxide phases (Casey, 2005; Casey et al., 2005; Oliveri et al., 2016; Wang et al., 2011). Aluminosilicates and clays, for example, are important sources of aluminum in soils (Abeysinghe et al., 2012). In the case of aluminum cations (Al^{3+}), the following mononuclear hydrolysis products are formed: $[Al(H_2O)_6]^{3+}$, $[Al(H_2O)_5(OH)]^{2+}$, $[Al(OH)_4]^-$ (Mesmer and Baes, 1990). Although the existence of oligomers in water has been suspected for decades, only a few of them have been synthesized and

crystallized (Casey et al., 2005). The number of possible complexes is higher when polynuclear complexes are formed compared to mononuclear complexes (Sillén, 1954). Although the interpretation of the results obtained depends on the methods used in the preparation and identification (Bottero et al., 1980), the aging time, for example, is considered important for hydrolyzed aluminum solutions because, although the initial steps are fast, condensation reactions become slower as the polynuclear cations become larger. At this point, change occurs slowly with time and depends on aluminum cation speciation, as well as counterions and heterospecies (Wood et al., 1990).

Hydroxide-containing molecules can be placed into two separate classes. The first of these comprises a Keggin-type structural arrangement characterized by central metals tetrahedrally coordinated to oxygen atoms (MO_4), encompassed by octahedra with common edges (Casey, 2005; Casey et al., 2005; Wang et al., 2011). These species are commonly obtained in aqueous solutions upon titration with a hard base and are considered to undergo rapid hydrolysis (Corum et al., 2015; Fairley et al., 2012). The second class of oligomers was discovered more recently and exhibits a characteristic core of edge-shared octahedra, which are organized into cubane-like moieties that are linked together (Casey, 2005; Casey et al., 2005). These species result in an acidic solution oxidizing metal or accompanied by chelating ligands, and are considered to undergo slow hydrolysis (Fairley et al., 2012). The Keggin-type species formation process is mostly governed by the ratio $[NaOH_T]/[Al_T]$ (total sodium hydroxide concentration/total aluminum concentration) (Brosset, 1952). In this regard, Sillen's "core + links" theory, which is related to this neutralization ratio (r = [NaOH]/$[Al_T]$), has been used by many authors to interpret their results in an acidic medium in terms of Al^{III} (Bottero et al., 1982). Brosset et al. (1952, 1954), for example, used potentiometric titration methods to study aluminum complexes while limiting the ratio r = [OH]/[Al] to 2.5. The composition of the resulting complexes agreed with the said theory. Similarly, Bottero et al. (1980, 1982) also used the potentiometric titration method, hydrolyzing solutions of aluminum chloride with sodium hydroxide while varying the ratio r = $[OH]/[Al_T]$ in dilute solution ((Al_T) =

10^{-1} mol/dm^3) at a temperature of 25 °C. Using ^{27}Al NMR spectroscopy, these authors reported the presence of five species, namely three monomers [$(Al(H_2O)_6]^{3+}$, $[Al(H_2O)_5(OH)]^{2+}$ and $[Al(H_2O)_4(OH)_2]^{+}$), a dimer [$(Al_2(OH)_2]^{4+}$), and the three-dimensional polymer Al_{13}, which has spherical symmetry (Bottero et al., 1980), that had previously been reported by Johansson (1960) and Akitt (1972). They also studied the variation in the percentage of aluminum bound in the various species as a function of the ratio r and the pH, as shown in **Figure 3** (Bottero et al., 1980). In 1982, Bottero et al. used small-angle X-ray scattering (SAXS) to investigate the effect of aging as well as particle shape and structure, finding that the colloidal species' particle morphology changes as a function of time. The distribution curve in **Figure 3** is dependent on the preparation method and shows that monomeric forms are dominant in the solution if OH/Al < 1. If the OH/Al value increases to between 1.5 and 2.3, the main species in solution is Al_{13}, and an increase in the degree of hydrolysis in the solution increases polymer formation (Cool and Vansant, 1998; Fu et al., 1991).

Rakotonarivo et al. (1984) studied the adsorption of sodium tetradecylsulfonate and sodium dodecylsulfonate on three aluminum hydroxide gels (r = [OH]/[Al_T] = 0, 2, and 2.5) at various pH values. These authors used the relationship between the molecular area of the absorbed ion, Avogadro's number, and adsorption isotherm data to calculate the surface area of these aluminum hydroxide gels at a pH of 6.5 and 7.5 in dilute solution ((Al_T) = 0.1 mol/dm^3). The resulting calculated surface areas varied from 500 to 1200 m^2/g and were found to decrease with increasing pH and [OH]/[Al_T] ratio. Mesmer and Baes (1990) published a review of the hydrolysis behavior of ions, including aluminum, and Casey et al. (2001) published a chapter which reviewed polynuclear complexes of aluminum. The various polynuclear species formed during the aqueous hydrolysis of aluminum depend on the tendency of the metal to hydrolyze, which in turn is reflected in the first hydrolysis reaction of the metal cation (Furrer et al., 1992; Mesmer and Baes, 1990). In the case of aluminum, which is an amphoteric element, it is known that, in aqueous solution, at least some of it is readily hydrolyzed in the pH range from 3 to 11 to form polynuclear

species referred to as “hydroxo polymers”, “hydroxo complexes”, or “polycations” (see *Supplementary Material*) (Bottero et al., 1980; Corum et al., 2015; Wood et al., 1990).

The work by Mesmer and Baes (1990) includes the dependence of hydrolysis on the temperature and distribution of Al^{III} hydrolysis products as a function of pH at Al^{III} concentrations of 0.1 and 10^{-5} mol/dm^3. These authors showed how the tendency of a few cations, including Al^{3+}, to hydrolyze increases with temperature (lower pH). This tendency is more pronounced in the case of Al^{III}, in which a starting temperature of 25 °C was observed at a pH of about 5 or lower. For a trivalent cation, saturation occurs at close to pH = 6 (slightly less than 6 at 100 °C and slightly higher at 25 °C), with the presence of $M(OH)_4^-$ being observed at higher pH values (Mesmer and Baes, 1990). Similarly, Brosset (1952) reported that, close to the point of equivalence, the viscosity of the solution reaches a maximum and its opalescence is flatter. Below pH = 3, aluminum exists exclusively as monomeric $[Al(H_2O)_6]^{3+}$, whereas above pH = 11 it is present as the $[AI(OH)_4]^-$ ion (Wood et al., 1990). This means that there are two processes which depend on the pH: one in the acid range and the other in the alkaline range (Brosset, 1952). The total aluminum concentration is important because the system becomes much more complex when it is increased (Wood et al., 1990). Brosset et al. (1952) assumed a primary protolysis with subsequent “protolytic association” for both environments (alkaline and acid). However, protolysis in an alkaline environment could directly result in the $[Al(OH)_4]^-$ ion, which contrasts with what occurs in an acidic environment, where the main ions formed are $[Al(H_2O)_5(OH)]^{2+}$ and $[Al(H_2O)_5(OH)_2]^+$. These latter ions may subsequently undergo proteolytic association, in which these and Al^{3+} ions may participate. If the aluminum ion is in an alkaline environment, it is protolyzed instantaneously to $[Al(OH)_4]^-$. If there is a sufficient excess of alkali in the solution, all the aluminum in it is immediately obtained as $[Al(OH)_4]^-$ and equilibrium prevails, rapidly reaching a constant pH value (Brosset, 1952).

When the pH is lower than 3 in an aqueous solution, the hydrated Al^{3+} cation is the primary species present. However, when the pH is increased, the monomeric species $[(Al(H_2O)_5OH)]^{2+}$, $[(Al(H_2O)_5(OH)_2)]^{+}$, and $[(Al(OH)_4)]^{-}$ condense to produce dimers $[(Al_2(OH)_2)]^{4+}$, trimers $[(Al_3(OH)_4)]^{5+}$, and a longer list of complex polymeric species, such as $[(Al_6(OH)_{15})]^{3+}$, $[(Al_7(OH)_{17})]^{4+}$, $[(AlO_4Al_{12}(OH)_{24}(H_2O)_{12})]^{7+}$, $[(Al_{16}(OH)_{38})]^{10+}$, $[(Al_{30}O_8(OH)_{56}(H_2O)_{24})]^{18+}$, $[(Al_9(OH)_n)]^{(27-n)+}$, etc. These include the tridecamer species ε-Al_{13} ($[Al_{13}O_4(OH)_{24}(H_2O)_{12}]^{7+}$) (Abeysinghe et al., 2012; Corum et al., 2015; Wu et al., 2016). Only a few of these aluminum-containing oligomers have been isolated, and only a limited amount of structural data are available (Casey, 2005; Wang et al., 2011). A large number of these polymers therefore remain uncharacterized and unidentified, partly due to the fact that ^{27}Al NMR spectroscopy only detects complexes with a tetrahedral site (Casey, 2005).

Kinetic phenomena in the hydrolysis process are pertinent because they have also been emphasized in some studies (Bottero et al., 1980). Thus, Brosset (1952) concluded that the reaction of aluminum in an alkaline aqueous environment is a first-order reaction, whereas in an acid environment it is a second-order reaction. This is related to the aging process and the formation of α-gel or products, respectively. Similarly, Casey (2005) reported kinetic aqueous interactions of the known aluminum hydroxide polyoxocations. In addition, these authors were pioneers in researching exchange kinetics involving Keggin-type species, using them to research similar reactions such as on extended mineral surfaces.

3. Al_{13} and Al_{30} formation

Al_{13} and Al_{30} structures are explained in the *Supplementary Material*. Polynuclear aluminum species can form naturally. Thus, Furrer et al. (1992) simulated natural conditions in the laboratory and found that the total aluminum concentration affects the formation of Al_{13}, with high concentrations favoring this formation and lower concentrations shifting formation to higher pH. For example, according to the equilibrium calculations, Al_{13} formation at an $[Al(III)]_T$ concentration

of 10^{-3} mol/dm^3 starts at pH = 4.2, whereas this process starts at a pH of between 5.0 and 6.0 at 10^{-5} mol/dm^3. At concentrations below 10^{-5} mol/dm^3, this transformation to Al_{13} is unlikely. These authors also reported that energetic stirring is not necessary and that more than 67% of the Al monomers were converted into Al_{13} polycations. The polymer maintains its +7 charge at a pH of less than 6 but loses nearly all its positive charge at a pH of between 6 and 7, after a series of deprotonation steps, which lead to the formation of species such as Al_{13}^{5+}, Al_{13}^{3+}, and Al_{13}^{+} (Abeysinghe et al., 2013b; Cool and Vansant, 1998; Vaughan, 1988). At a pH above 6, the equilibrium conditions are totally altered and aggregation due to proton loss from Al_{13} occurs (Mertens et al., 2016). Other complexes are also found in solution as a result of the interaction between dissolved metal cations and the partially neutralized Keggin ions (Furrer et al., 1992). The acidity is important to obtain good control of the charge of the Al_{13} polyoxycations because the OH/Al ratio is directly related to the pH of the solution (Cool and Vansant, 1998). In this regard, Vaughan published a study of the charge variation due to pH, showing that, as the pH increases, the charge decreases, and considering the possibility that, in solution at pH > 3, polymers with no less than two different charges are likely to be present (Vaughan, 1988).

Nazar et al. (Fu et al., 1991; Nazar et al., 1992) studied the hydrolysis of aluminum in an aqueous solution at high temperatures (80 – 95 °C) and identified three new polyoxoaluminum cations (denoted as AlP_1, AlP_2, and AlP_3) formed by thermal transformation of the tridecamer cation Al_{13} after aging for a few days. Using kinetic NMR analysis and quantitative NMR studies, these authors proposed that the first step in the thermal evolution involves degradation of the tridecamer cluster (Al_{13}), which loses one octahedral Al unit to form the intermediate species AlP_1 (Al_{12}, a defective Al_{13} structure). This species contains four active sites and react via condensation/polymerization to form larger and more stable polycationic species. The next step is the dimerization of two AlP_1 species to form the AlP_2 cluster, tentatively formulated as $Al_{24}O_{72}$, which is transformed into AlP_3 upon further heating, despite being stable in solution. This transformation involves distortion of

the Al-tetrahedral sites (Fu et al., 1991; Nazar et al., 1992) (**Figure 4**). The transformation of Al^{III} into Al_{13} and then AlP_2 is favored by hydrolysis (OH/Al = 2.25) of $AlCl_3$ solutions (0.25 mol/dm^3) at 80 °C. Thus, Parker et al. (1997) aged a solution recently titrated with a base at 80 °C and found that the conversion from Al_{13} into AlP_2 was faster than reported by Fu et al. (1991), who studied a "pure" Al_{13} solution aged at 85 °C. We now know that the AlP_2 species identified by Nazar et al. (Fu et al., 1991; Nazar et al., 1992) corresponds to the Al_{30} molecule [Al_{30} = $Al_2O_8Al_{28}(OH)_{56}(H_2O)_{26}{}^{18+}{}_{(aq)}$] (Casey, 2005).

Allouche and Taulelle (2003a) demonstrated that Al monomers $[Al(H_2O)_6]^{3+}$ control conversion of the ε-Al_{13} Keggin species into Al_{30} by ^{27}Al NMR spectroscopy. Indeed, the presence thereof in solution is crucial to this synthesis. These authors also proposed the chemical pathway illustrated in **Figure 5** to explain the thermal isomerization process: ε-Al_{13} and one aluminum monomer form an intermediate species, ε-Al_{14}, which isomerizes into δ-Al_{14} at high temperatures. The Al_{30} cluster then forms via a new dimerization and reaction with two other monomers. Allouche and Taulelle also published a paper (2003b) in which they enhanced the formation of Al_{30} polycations and other new Keggin isomers by fluorinating the Al_{13} polycation, partially substituting the di-μ_2-OH bridges with fluorides. Barriers have to be overcome in order for ε-Al_{14} to isomerize into δ-Al_{14} repulsive electrical energy, thus making the temperature pertinent to the formation of Al_{30}. In this regard, temperatures ranging from 70 to 125 °C have been reported in the literature (Ye et al., 2013). Allouche and Taulelle (2003a) demonstrated that the temperature is not essential to produce Al_{30}. Indeed, these authors reported the involuntary production of Al_{30} by aging an Al_{13} solution at 20 °C. However, an increase in temperature accelerates the conversion of Al_{13} into the Al_{30} species. One example of this would be heating it for 48 h at 95 °C or 5 h at 125 °C; in addition to the monomer content and heating time, the cumulative Al concentration (AlT) also affects the conversion by facilitating it with lower concentrations and longer aging times (Ye et al., 2013).

Several studies have proposed that δ-Al_{13} is a necessary unit for polymerization of the ε-Al_{13} cluster into larger polymeric species, including Al_{30}, which is formed by two δ-Al_{13} species joined via four octahedrally coordinated Al^{3+} cations located in the central region (Abeysinghe et al., 2013a; Abeysinghe et al., 2013b). However, the mechanism for the transformation of Al_{13} into Al_{30} and the energy implied in this process is not completely understood due to the complexity of the proposed steps and the fact that intermediate products are difficult to detect (Ye et al., 2013). Additionally, the calculated energy required for the rotation step in the isomerization process is too high to explain the experimental observations (André Ohlin et al., 2014; Oliveri et al., 2016), as shown in the *Supplementary Material*.

The Al_{13} cluster, which is considered the direct precursor to Al_{30}, is affected by pH, with aggregation occurring at a pH higher than 6 (Allouche and Taulelle, 2003a; Furrer et al., 1992; Mertens et al., 2016; Shafran et al., 2004; Shafran and Perry, 2005), as mentioned in previous sections. Ye et al. (2013) studied the effect of these alkali-induced Al_{13} aggregates and Al monomers on Al_{30} formation at high temperature, using ^{27}Al NMR spectroscopy and dynamic light scattering (DLS) measurements. These authors also reported that Al_{13} aggregates affect Al_{30} formation, which increases with aging and decreases upon addition of a base. Similarly, Chen et al. (2005) studied the effect of total aluminum concentration on the formation of Al_{13} and its transformation into Al_{30} in an aqueous solution. These authors reported that the rate of conversion of Al_{13} into Al_{30} increases markedly as the total Al concentration increases and that, when higher than 0.75 mol/dm^3, the Al_{30} cluster content increases continuously, becoming predominant in a fresh polyaluminum solution heated at 95 °C for 12 h.

Shafran et al. (2004, 2005) studied Al speciation at high temperature (90 °C) for a range of hydrolysis ratios and pH levels by potentiometric titration, ^{27}Al NMR spectroscopy, and DLS. The speciation diagrams of Al-ion hydrolysis as a function of pH and hydrolysis ratios are shown in **Figure 6** for several hydrolysis times. **Figure 6** shows that, at a pH of less than 4 (range considered highly acidic), Al

monomers are the majority species, whereas Al dimers appear at pH < 4.3, although their concentration never exceeds 34% of soluble Al species and, thus, they are considered less important. Additionally, these authors found that the quantity of Al_{13} decreased as the quantity of Al_{30} increased, reaching a maximum concentration at a pH of around 5.0–5.5 when heated at 90 °C for 12 and 24 h (Shafran et al., 2004). For short periods of hydrolysis (1 and 3 h), Al_{13} and Al_{30} are the predominant species in solution at a pH of roughly 4-6, which corresponds to the approximate hydrolysis ratio range $1.6 \leq h \leq 2.6$. However, at longer hydrolysis times (>6 h), Al_{30} is the predominant species (Shafran and Perry, 2005).

Sulfate and selenate anions, and various solid-state techniques, have commonly been used to isolate and characterize both Al_{13} isomers and larger Al-cations (Abeysinghe et al., 2013a). Thus, since 1991, the structures of larger Al-cations such as Al_{26}, Al_{30}, and Al_{32} ($[Al_{26}O_8(OH)_{50}(H_2O)_{20}]^{12+}$, $[Al_{30}O_8(OH)_{56}(H_2O)_{26}]^{18+}$, and $[Al_{32}O_8(OH)_{60}(H_2O)_{28}]^{20+}$ respectively) have been characterized and found to contain two δ-Al_{13} species. However, the most widely studied cluster has been Al_{30}, which is now well characterized (Abeysinghe et al., 2012; Allouche et al., 2000; Allouche and Taulelle, 2003a; Fu et al., 1991; Oliveri et al., 2016; Phillips et al., 2003; Rowsell and Nazar, 2000; Sun et al., 2011). The importance of temperature as regards both the formation and transformation of Al_{13} and Al_{30} species has also been studied. Thus, Chen et al. (2007) used highly concentrated hydrolytic polymeric Al solutions (HPA) to study this effect. These authors reported that, in fresh solutions, the Al_{13} cluster was the primary component, but that this situation changed when the solution was heated to 95 °C, where the Al_{30} content increased to become the predominant component after heating at that temperature for 12 h. Due to the relevance of supramolecular chemistry in the field of separation science, some authors have successfully applied this approach to crystallization in the synthesis and structural characterization of Al_{13} and Al_{30} Keggin-type aluminum clusters in aqueous solutions. To isolate the ε-Al_{13} cluster, Drljaca et al. (1999) used *p*-sulfonatocalix[4]arene, whereas Mainicheva et al. (2006) used cucurbit[6]uril to isolate Al_{30}. This latter species was also studied by Abeysinghe et

al., (2012) who used 2,6-naphthalene disulfonate (2,6-NDS) to improve crystallization using the supramolecular approach and similarly, crystallized the intermediate species in the solution, reporting δ-Al_{13}, Al_{26}, and Al_{30}. These authors observed that the Al_{26} polycation comprises two δ-Al_{13} clusters, which are polymerized via the vertex-sharing of two hydroxyl groups. Al_{26} is an intermediate product in the transformation of ε-Al_{13} into larger polynuclear species. **Figure 7** shows the formation mechanism for large polymeric species such as Al_{26}, Al_{30}, and Al_{32}S and illustrates how the ε-Al_{13} isomer, which is the majority species in solution at a pH of between 3 and 5, is converted into δ-Al_{13} upon aging or heating. This cluster is linked to additional monomeric species that form the aforementioned larger polymeric structures. The δ-Al_{13} isomer could be considered to be the building block of larger polymeric species upon heating or aging (Fairley et al., 2012). This molecule also contains a capping sodium atom (see *Supplementary Material*). This atom appears to stabilize the δ-Al_{13} cluster shortly before its polymerization into larger aluminum polycations. Removal of the sodium atom results in formation of the Al_{26} polycation, which is very likely an intermediate product. Higher hydrolysis ratios imply a lower presence of aluminum monomers and dimers in solution, thereby favoring the formation of Al_{26} rather than Al_{30} and Al_{32}S species (Abeysinghe et al., 2012).

The complete mechanism for Al_{13} and Al_{30} formation published by Wen et al. (2019a) is presented in **Figure 8**. It can be seen that the step following monomeric species formation at 60 °C in the hydrolysis process (a.1) is the aggregation of these species via the reactions shown in supplementary material to form dimers (a.1) and trimers (a.2), followed by the Al_{13} polycation (a.4). This Al_{13} formation is controlled by the temperature and aging process (OH/Al ratio = 2.4 and a final pH of 3.93). **Figure 8b** represents equation 7, which shows how the ε-Al_{13} initially dissolves and subsequently rearranges to the δ-Al_{13} isomer, then how two δ-Al_{13} species can be linked to four monomers to form Al_{30} (pH solution = 4.21) under appropriate conditions such as high temperature (95 °C in an oil bath). The active sites in the Al_{13} structure have been studied, finding similarities between the oxygen atoms in its

structure (Bradley et al., 1993; Casey et al., 2000; Wehrli et al., 1990). Thus, Casey et al. (2000) employed ^{17}O NMR spectroscopy to study the oxygen exchange rates between the “O” and “OH” sites in Al_{13} using ^{17}O-enriched water. These authors found that, of the two inequivalent μ_2-OH bridges (inter- or intra-trimer) in the ε-Al_{13}, referred to as μ_2-OH^a and μ_2-OH^b (see *Supplementary Material*), μ_2-OH^a is the most labile hydroxo site. The transformation of ε-Al_{13} into δ-Al_{14} is possible because of the lability of the μ_2-OH^a bridges, with the former being capped with Al^{III} monomers (Allouche and Taulelle, 2003b; Wen et al., 2019a). This scheme shows the importance of the monomeric species, in accord to the conclusions published by Allouche and Taulelle (2003a) and Ye et al. (2013). An excess of monomer in solution is necessary for two reasons: 1) they are the basic units that form and connect δ-Keggin-Al_{14} and form Keggin-Al_{30}, and 2) because they facilitate Al_{30} formation by increasing the dissolution rate of ε-Keggin-Al_{13}, which promotes the rearrangement and isomerization processes, how was shown by Yang et al. (2010) who investigated the formation mechanism of Al_{30} using density functional theory. Similarly, Ye et al. (2013) studied the effect of monomeric Al on Al_{30} formation, as well as the influence of Al_{13} aggregates, obtained upon alkali addition or aging. These experiments were carried out under high temperatures (95 °C) using characterization techniques such as DLS and ^{27}Al NMR spectroscopy. These authors found that Al_{13} is also a necessary precursor in the formation of Al_{30}, and that this formation is faster and gives higher yields when Al_{13} aggregates are formed by aging rather than by titration.

In conclusion, the polymerization of Al_{13} to Al_{30} can be achieved by long term aging or additional heating (127 °C for 5 h, or 95 °C for 48 h) of a concentrated Al_{13} solution (Abeysinghe et al., 2013b; Mertens et al., 2012; Ye et al., 2013). This reaction can be enhanced using an autoclave, thus resulting in a high yield of Al_{30} (Motalov et al., 2017). Moreover, $Al(OH)_3$ formation in Al_{13}-containing solutions is not a problem because the formation of the Al_{13} polymer is significantly faster than the precipitation of $Al(OH)_3$ phases (Furrer et al., 1992).

4. Acidity and reactivity

As a result of the hydroxide ions and water groups in the structures, both Al_{13} and Al_{30} exhibit high reactivity (Mertens, 2011). Thus, both undergo deprotonation over a broad pH range and exhibit a highly stable structure, nanoscale molecular size, a large surface area, and a high surface charge (+7 and +18 respectively) depending on the [OH]/[Al] ratio and pH (Bottero and Bersillon, 1988; Casey, 2005; Furrer et al., 1992; Mertens, 2011; Rakotonarivo et al., 1984; Wu et al., 2016; Ye et al., 2013). However, the particle size of Al_{30} is nearly twice as large, and its positive net charge is more than 2.5 times higher (Wen et al., 2019a). Al_{30} is also more acidic than its precursor (ε-Al_{13}) as a result of acidic η-H_2O functional groups, as published by Rustad (2005), who calculated the relative degree of protonation of Al_{30} and was the first to use molecular dynamics simulations of an acidimetric titration. The deprotonation of Al_{13} starts at pH = 6, as mentioned in preceding sections, and the results obtained for both Al_{13} and Al_{30} clusters are similar. One difference between them was observed in the slope of their titration curves, which is steep for ε-Al_{13} and more gradual for Al_{30}. This indicates that the initial deprotonation events are defined, reaching neutralization when the pH of the solution is approximately 6.7 (pH of zero charge, pH_{PZC}) (Abeysinghe et al., 2013b). Al_{30} deprotonates in the pH range 4 to 7 (Rustad, 2005), and its high reactivity is due to the large number of OH^- and H_2O groups (Mertens, 2011). Rustad (2005) published a theoretical study of the reactivity of Al_{30} using molecular dynamics simulations and keeping the notation and group numbering used by Casey et al. (2001). A scheme with the oxygen functional groups in Al_{30} and Al_{13} is included in **Figure 9**. Al_{13} contains twelve identical water molecules (η-H_2O) (9a), and two types of μ_2OH bridging groups (between dimeric or trimeric groups) (9b). Similarly, Al_{30} contains 26 bound terminal water molecules (η-H_2O), which can be divided into five groups depending on their proximity to the central region where both δ-Keggin isomers are linked (9c), 50 doubly bridging (μ_2-OH) ligands, and six triply-bridging (μ_3-OH) ligands (9d) (Casey et al., 2001; Rustad, 2005). Rustad (2005) also reported that the two 4-ηH_2O groups are the most acidic groups in the Al_{30} molecule and, after deprotonation, form $H_3O_2^-$ ligands with the two 3-ηH_2O groups. A strong coupling of these sites was also observed.

In 2013 and 2015, Forbes and coworkers published three studies in which they combined theoretical and experimental research. In the first (Abeysinghe et al., 2013b), these authors synthesized and characterized two models of Al_{30} modified with chelated metal centers (Al^{III} and Zn^{II}), using an iminodiacetic acid (2,6-NDS, IDA) and nitrilotriacetic acid (NTA), respectively (Al_{32}IDA and Zn_2Al_{32}NTA). They found that the reactivity in their experimental models of Al_{30} accord to the reactive sites predicted by molecular dynamics simulations. In their second paper (Abeysinghe et al., 2013a), they studied the adsorption of Cu^{2+} on the surface of Keggin-type polyaluminum species (Cu_2Al_{30}-S) crystallized in the presence of disulfonate anions, exploring the adsorption process using density functional theory (DFT). Their results suggested that the reactivity of Al_{30} toward anions and cations differs, with anions preferring the beltway and cations preferring the caps of the Al_{30} structure. This study is shown in **Figure 10a**, where the red surfaces represent regions with higher values of electrostatic potential (highest in the beltway) and the blue surfaces represent regions with lower values (lowest at the caps). In the third paper (Corum et al., 2015), these authors used $(TBP)_2Al_{30}$-S (TBP = t-butylphosphonate) as a model to study the reactivity of oxyanions with aluminum hydroxide surfaces. They found that the beltway region of Al_{30} is the most reactive and that preferential binding of phosphate occurs in this region. Al_{30}^{16+} ($[Al_{30}O_8(OH)_{58}(H_2O)_{24}]^{16+}$) was used as the initial form in the adsorption modeling using DFT vibrational calculations, finding that Al_{30}^{18+} ($[Al_{30}O_8(OH)_{56}(H_2O)_{26}]^{18+}$), which is the molecular formula expected of Al_{30}, is unstable. These findings support the results obtained by Casey and Rustad (2005b), using perchlorate anions (**Figure 10b**), who found that the belt region has the highest acidity in Al_{30} as the highest deprotonation occurs in this region.

5. Al_{13}- and Al_{30}-PILC montmorillonites

Since the 1970s, when the first family of aluminum intercalated clays was reported, PILC have attracted increasing interest from the scientific and industrial

sectors. Several patents have also been granted for such compounds, including three granted to Vaughan, Lussier, and Magee (all assigned to W.R. Grace and Co.), covering the concept of pillaring using specific inorganic polymers (Cañizares et al., 1999; Gil et al., 2000a; Vaughan, 1988; Wen et al., 2019a; Zhu et al., 2017). In 1988, Vaughan published “Pillared clays - historical perspective”, in which he described the patents mentioned (Vaughan, 1988). The first report of the structure of ε-Al_{13} was published in 1960 by Johansson (1960), and the first reports of pillared clays using montmorillonite and Al_{13} polycations appeared in the period 1977–1981 (Gil et al., 2000a). Since then, several studies that attempt to understand and improve the properties of pillared clays have been published. Various reviews in this field have tried to bring together the extensive published information regarding the synthesis and characterization of PILC, their application in catalysis and adsorption, and the techniques used to characterize them (Baloyi et al., 2018; Ding et al., 2001; Gil et al., 2000a; Gil et al., 2011c; Gil et al., 2008; Kausar et al., 2018; Kloprogge et al., 2005; Kloprogge, 1998; Lazaratou et al., 2020; Ngulube et al., 2017). The majority of studies on PILC involve Al_{13}, although in some cases this is simply an inference due to the experimental conditions utilized. However, under thermal conditions, the Al_{13} cluster is normally converted into another species. This means that a large proportion of the papers published may actually have used a mixture of Keggin-clusters (including Al_{30}) or clusters larger than Al_{13} as an intercalating solution in which the Al_{13} species may be only a minor component or even absent (Parker et al., 1997; Smart et al., 2013). The use of Al_{30} in this field has received little attention even though its characteristics make it an appropriate intercalant that can improve the characteristics of the PILC (Wen et al., 2019a; Zhu et al., 2017).

The characteristics of Al-PILC montmorillonites, including their pore size distributions, surface areas, and surface acidities, can change depending on the preparation procedures and affect their applications, as concluded by several authors such as Mokaya and Jones (1993), Sterte and Otterstedt (1987), Matsuda et al. (1988), Trillo et al. (1993), and Moreno et al. (1997). Similarly, Zuo and Zhou (2008) found a relationship between the pore structure of Al-PILC and the conditions

used in its synthesis. These authors also studied the relationship between the structure of these materials when used as a support in the catalysis of benzene oxidation and their catalytic properties in this process. Gil et al. (2008) reviewed studies related to the control of the microstructure in Al-PILC, including controlling characteristics by adjusting the different parameters in the synthesis process. This review shows how the characteristics of PILC depend on the size, chemical nature, and number of intercalated species, among other aspects, and that modification of the thermal step can affect both the interpillar and interlayer spacings. The type of species formed, which differ in terms of size and net charge, depends on the experimental parameters used. Temperature and pH were two factors mentioned in the "Al_{13} and Al_{30} Formation" and "Aluminum Hydrolysis" sections.

Pinnavia et al. (1984) compared the physical and catalytic properties of PILC obtained using natural and synthetic smectite. Cañizares et al. (1999) also compared PILC prepared commercially and naturally (bentonites) with single (Fe, Cr or Zr) and mixed-oxide pillars (those metals and aluminum) and observed larger basal spacings and surface areas in PILC prepared from commercial bentonite than in those prepared from natural bentonite, which may be related to the higher crystallinity of the commercial bentonite used. The incorporation of aluminum into the single oxide enhanced the thermal stability, surface acidity, and methane adsorption. However, the Al/metal ratio used also played an important role by affecting the pillar structure, with higher values making the Keggin structure predominant. Although the basal spacing of the clay is 0.96 nm, its pore size normally ranges from 1.8 to 2.0 nm after insertion of the Keggin-type polycations. Accordingly, the pore size openings in the PILC depend on the size of the polycations (Cañizares et al., 1999); changing the nature and, therefore, the pillar size results in different pore sizes in the PILC, thus making it possible to tune the porosity in such solids (Cool and Vansant, 1998; Maes et al., 1997). The dimensions of the Al_{13} Keggin structure were proposed in 1988 (Clearfield and Roberts, 1988) and found accord to the interlayer distance in the Al_{13}-PILC montmorillonite (0.8 to 1.0 nm) (Gil et al., 2008).

Butman et al. (2015) reported the structural and textural properties of some PILC obtained by intercalating montmorillonite with large Al (Al_{13} and Al_{30}) and Al/Ce polyhydroxo complexes. These authors reported an increase in the basal distance (nm) of the montmorillonite and in the surface areas (S_{BET}, m^2/g) due to an increase in polycation size from 1.26 (initial) to 1.64 (108 m^2/g), 1.88 (125 m^2/g), and 2.41 nm (147-154 m^2/g) for Al_{13}, Al_{30}, and Al/Ce pillars, respectively. Similarly, Zhu et al. (2017) also published an Al_{30}-PILC montmorillonite synthesis based on the method by Butman et al. (2015), which they considered to be a good attempt at such a synthesis despite the fact that the results published by the latter do not show an obvious enhancement in the properties and that this method also involves a complicated hydrothermal process. For this reason, Zhu et al. (2017) announced theirs was the first successful reported synthesis of an Al_{30}-PILC montmorillonite. These authors used characterization techniques such as X-ray diffraction (XRD), X-ray fluorescence (XRF), ^{27}Al NMR spectroscopy, transmission electron microscopy (TEM), and nitrogen adsorption-desorption isotherms, and obtained solids with surface areas (S_{BET}) of 70 (clay mineral), 259 (Al_{13}-PILC), and 311 m^2/g (Al_{30}-PILC), which show a clear enhancement in the properties. Furthermore, they reported an increase in the $(Al_2O_3)/(SiO_2)$ ratio from 0.27 (clay) to 0.46 (Al_{13}-PILC) and 0.60 (Al_{30}-PILC). The Al_{30}-PILC formation process published by Zhu et al. (2018) is presented in **Figure 11**, which shows how two adjacent Al_{30}-cluster arrangements in the interlayer of the montmorillonite can create a more sizeable pore. As a future challenge, these authors proposed a change in the orientation of Al_{30} pillars from horizontal to vertical, thus resulting in PILC with a higher microporosity and larger interlayer spacing, thereby furthering their applications as catalysts and adsorbent materials. Gil and Vicente (2020) considered that a future challenge in the synthesis of PILC could be to explore new structures and find new sources of polycations, including the use of wastes such as industrial metal wastes. Other challenges include their reuse and adaption for specific applications by designing and controlling the porous structure.

6. Use of both Al_{13} and Al_{30} polycations as intercalating agents in PILC

Keggin-type polyaluminum clusters are well-defined species that have been extensively characterized over the last six decades (Abeysinghe et al., 2013a), as discussed previously. These substances are environmentally significant and have been used in various fields. For example, they are considered essential in industries that release large quantities of organic compounds into wastewater, such as the paper industry. They are generally used as flocculants or to form cationic sols for the adsorption of organic compounds in water by adding industrial chemicals such as aluminum chlorohydrate or polyaluminum chloride, which comprise ε-Al_{13}, and Al_{30} (Bottero and Bersillon, 1988; Casey, 2005; Phillips et al., 2016). The hydrolysis/precipitation behaviors (Al^{III}, Al_{13}, and Al_{30}) and use of Al_{30} species as a coagulant to enhance turbidity removal have also been studied (Chen et al., 2006; Chen et al., 2009), as has their application in the uptake of heavy metals such as arsenic during water treatment (Mertens, 2011; Mertens et al., 2012; Mertens et al., 2016). In addition to their use as water-clarifying agents, polyaluminum Keggin-type species are also used as pillaring agents in the synthesis of pillared clays (PILC) from layered clays. They are also precursors for heterometallic catalysts upon deprotonation of their amphoteric functional groups, which is related to their ability to adsorb a range of inorganic and organic species on their surfaces (Abeysinghe et al., 2013b; Rowsell and Nazar, 2000).

As mentioned in the Introduction section, the procedure for synthesizing pillared clays can be understood to involve two main steps, (**Figure 2b**): intercalation and calcination. **Figure 12** shows a simple scheme of the general process for synthesizing PILC. The first step involves the preparation of the intercalating solution. One of the most common inorganic intercalating agents for clays is ε-Al_{13} (Casey, 2005). Indeed, Cool and Vansant (1998), in a chapter of "Synthesis. Molecular Sieves", cited four general methods for the preparation of Al-intercalating solutions to form the Keggin-Al_{13} polycation, namely two possible hydrolyses of Al^{III} salts, using $AlCl_3$ and a strong base (NaOH) or with Na_2CO_3, electrolysis of $AlCl_3$, or

the dissolution of Al metal in HCl. The first method is the most widely used on a laboratory scale, and the latter on an industrial scale, producing concentrated hydrolyzed Al solutions, such as *Locron* (4.6 mol/dm^3), which can be used as the intercalating solution if diluted to reach the same concentration, OH/Al ratio, and pH used in the first method (Cool and Vansant, 1998). The use of these commercially available chemicals has been studied in both pillared clays and water treatment, sometimes comparing their use to that of pure Al_{13} and Al_{30} solutions (Mertens et al., 2016; Pinnavaia et al., 1984). The use of polyaluminum chloride (PAC) as a coagulant in water treatment is well known, and several studies relating to its coagulation mechanism, such as that by Wu et al. (2016), who compared polyaluminum chlorides with high Al_{13} and Al_{30} contents, have been published. Its use to remove contaminants has also been studied by Mertens et al. (2016), who compared arsenic uptake and its bonding sites in a few Al-based sorbents, including commercially available PAC and Al nanoclusters.

As regards its use in the PILC field, Pinnavaia et al. (1984), for example, made a comparison between the use of commercial diluted aluminum chlorohydrate (ACH) and the Al_{13} solution obtained upon hydrolysis of $AlCl_3$ with NaOH in the pillaring process. These authors showed that both these systems resulted in pillared products with similar characteristics, such as pore sizes and thermal stability, in addition to catalytic properties. Other researchers, such as Sterte et al. (1987, 1988), Mokaya and Jones (1993), Jones and Purnell (1993), and Polubesova et al. (2000), have also reported the use of ACH solutions in the intercalating process.

Use of the titration method to produce Al_{13} from a strong base and dissolved Al^{III} salts (normally NaOH and $AlCl_3$), with aging times of between 24 and 48 h after titration (Mertens et al., 2012). This process has been studied for a broad range of total aluminum concentrations (10^{-5} - 1 mol/dm^3), using a variety of techniques (Casey, 2005; Fu et al., 1991; Gil et al., 2011b) to study the polymers formed and the PILC obtained using these solutions.

Over the years, several authors have prepared Al_{13} intercalating solutions by hydrolyzing aluminum chloride by dropwise addition of a NaOH solution. A few of them, such as Lahav et al. (1978), Plee et al. (1987), Pesquera et al. (1991), and Hutson et al. (1999), have studied the effect of varying the $[OH^-]/[Al^{3+}]$ molar ratio. Thus, some groups have reported using this method with $[OH^-]/[Al^{3+}]$ molar ratios of 2.0 - 2.4 (pH = 4.0 - 4.7), followed by an aging time of 24 - 48 h at 50 – 60 °C (Bradley et al., 1990; Butman et al., 2015; Cool and Vansant, 1998; Gil et al., 2008; Gil et al., 2007; Gil and Montes, 1994c; Guerra et al., 2008; Wen et al., 2019a; Wen et al., 2019b; Wu et al., 2016; Zhu et al., 2018; Zhu et al., 2017; Zuo and Zhou, 2008), whereas others have used higher temperature titrations (80 – 95 °C) at similar $[OH^-]/[Al^{3+}]$ ratios (1.5 – 2.5) (Abeysinghe et al., 2013a; Abeysinghe et al., 2013b; Allouche et al., 2000; Allouche and Taulelle, 2003b; Casey, 2005; Corum et al., 2015; Gil and Montes, 1994a, b), some of them subsequently aging the resulting mixtures at room temperature, in some cases for 1 - 2 weeks. Allouche and Taulelle (2003a), for example, confirmed that it is possible to obtain a pure ε-Al_{13} solution by direct synthesis at an $[OH^-]/[Al^{3+}]$ molar ratio of 2.46 with an aluminum concentration of 0.5 mol/dm^3 at 100 °C by *in situ* ^{27}Al NMR spectroscopy. Others have studied the hydrolysis of aluminum chloride using similar $[OH^-]/[Al^{3+}]$ molar ratios (1.6 – 2.2), aging at room temperature for 24 h (Cheng and Yang, 1997; Gil et al., 2000b; Hutson et al., 1999; Molina et al., 1992; Moreno et al., 1997) and 1 - 4 weeks (Shabtai et al., 1984; Tokarz and Shabtai, 1985), or by aging at reflux temperatures in the range of 85 – 100 °C for short periods of between 3 and 48 h (Salerno et al., 2001; Tokarz and Shabtai, 1985; Trillo et al., 1993). Tokarz and Shabtai (1985) reported that PILC obtained under reflux were thermally more stable and also had higher porosity than those obtained at room temperature. This stability is possible because the pillars in these PILC are likely in bigger clusters than Al_{13} produced at high temperatures (Parker et al., 1997), as explained in the "Al_{13} and Al_{30} Formation" section.

Keggin-Al_{30} intercalating solution can be obtained using the hydrothermal technique, maintaining the Al_{13}-containing solution (obtained by hydrolysis titration or using a commercial solution) at high temperatures (Butman et al., 2015), or using higher temperatures in the aluminum hydrolysis titration procedure. For example,

authors have reported the use of 60 °C for 24 h (Motalov et al., 2017), 80 - 95 °C for 12 – 36 h (Corum et al., 2015; Wen et al., 2019a; Wen et al., 2019b; Wu et al., 2016; Zhu et al., 2018; Zhu et al., 2017), or a higher temperature for a shorter time (127 °C for 5 h) (Butman et al., 2015), stirring in all cases, and using an oil bath (Wen et al., 2019a; Wen et al., 2019b; Zhu et al., 2018; Zhu et al., 2017), refluxing (Wu et al., 2016) or a reactor (Butman et al., 2015; Corum et al., 2015). Other authors, such as Vogels et al. (2005) and Feng et al. (2007), have reported the formation of the Al_{13} polycation by thermal decomposition of urea. Similarly, Sivaiah et al. (2010) reported the use of microwave instead of conventional heating to assist the formation of aluminum polycations/oligomers, especially the Al_{13} polycation, in both conventional titration and thermal decomposition of urea. These authors used both polycation and oligomer solutions to prepare Al-PILC montmorillonites and found that those prepared using the oligomers formed during the breakdown of urea had a higher micropore volume and surface area. The presence of other Al oligomers higher than Al_{13} in the thermal decomposition of urea assisted by microwave heating was also observed.

7. Intercalation process

Once the intercalating solution has been prepared, it is used in the intercalation process to facilitate an ion-exchange reaction between the Al-Keggin ions (Al_{13} or Al_{30}) in the solution and the interlayer ions in the montmorillonite (Na^+) (Cool and Vansant, 1998), as mentioned in the Introduction section. The intercalating process requires both polycations and the parent clay to have certain properties. For example, the characteristics of the polycations in the solution, including the amount of positive charge and the charge distribution in their surface area, contribute to the exchange process (Wen et al., 2019a). In the case of the clay, the cation exchange capacity (CEC) is important because it is related to the quantity of pillars intercalated. Higher CEC values may mean that the clay charge is not fully compensated, especially if the polycations used have a low charge or are large. Lower CEC values imply that the clay will need only a few pillars to compensate for its charge, which

could signify ineffective intercalation, especially if the polycations used are highly charged or small (Gil et al., 2008). This was demonstrated in the study published by Suzuki et al. (1988, 1989), who compared Al-PILC prepared by varying the CEC of the montmorillonite. Other authors have also studied the pillar density in Al-PILC montmorillonites (Cheng and Yang, 1997; Gil et al., 2000b; Hutson et al., 1999; Suzuki et al., 1988; Suzuki and Mori, 1989). For example, Cheng and Yang (1997) and Hutson et al. (1999) compared the Al-PILC prepared using two montmorillonites with very different CECs (0.70 and 1.40 mequiv/g) and found that both PILC had almost the same interlayer spacings but differed in terms of pillar density. This was higher in the PILC with a higher CEC in the raw clay, which resulted in a lower microporosity in this PILC. A moderate CEC is therefore required, and smectites or TOT are ideal hosts, as mentioned in the Introduction section (Cool and Vansant, 1998).

The surface acidity of clay minerals is important in several processes and applications, including their use in heterogeneous catalysis (Lambert and Poncelet, 1997; Wen et al., 2019b). The surface acidity of montmorillonite, a TOT clay, arises due to its ability to donate protons, which is determined by the oxygen atoms of the Si tetrahedron in its basal structure. **Figure 13** shows possible acid sites in this clay, which has both Lewis and Brønsted acid sites (Wen et al., 2019b). Salerno et al. (2001) found that acidity is higher in PILC, and the strength and number of the acid sites formed in this process depend primarily on the Al/Clay ratio. PILC have both Lewis and Brønsted acid sites, with the ratio between them depending on the type of clay (Cool and Vansant, 1998). The relationship between the pillars and the change in surface acidic properties of the montmorillonite has also been studied (Bradley and Kydd, 1993; Casey, 2005; Wen et al., 2019b). Thus, Bradley and Kidd (1993) compared the acidic character of montmorillonite after pillaring with various tridecameric cations, including Al_{13} and $GaAl_{12}$, and found that the Lewis and Brønsted acidic sites in the resulting PILC depend on the pillars. These pillars affect the acidity mainly because their introduction into clays increases the interlayer spacing, microporosity, and surface areas, thereby exposing the acid sites in the

phyllosilicate sheet (Bradley and Kydd, 1993; Casey, 2005). After the intercalation process, hydrolysis of the Keggin ions continues to a degree that depends on the host type (Cool and Vansant, 1998).

To try to understand the behavior of Keggin polycations during the formation of Al-PILC, and how this is related to their improved properties, Wen et al. (2019 a,b) performed two studies of the relationship between the pillars, the surface acidity of the clay, and the formation and transformation of these pillars during the entire process (from hydrolysis to calcination). In the first study (Wen et al., 2019b), they demonstrated the effect of the pillars on the surface acidity of montmorillonite and their relationship to the Al/Si ratio by comparing the catalytic oxidation of toluene using montmorillonite and Al_{13}- and Al_{30}-PILC montmorillonites. To study the impact on surface acidity when the montmorillonite was pillared using Al_{13} and Al_{30}-Keggin polycations, they used NH_3-TPD (NH_3 temperature-programmed desorption) and NH_3-adsorbed DR-FTIR (NH_3-adsorbed diffuse reflectance Fourier transform infrared). This study showed that it is possible to propose arrangement models for these polycations in the interlayer space of the clay mineral (**Figure 14**) based on the results obtained, including the results of powder XRD and the chemical composition and structural parameters of the clay mineral. These authors also found that both Al_{13}- and Al_{30}-PILC showed an increase in surface acid sites, mainly Brønsted acid sites (both strong and weak), although the number of these sites depended on the Al/Si ratio. A high catalytic activity was reported for Al_{30}-PILC at a much lower temperature than for the others. Particle sizes of approximately 0.9 × 0.9 × 0.9 (Keggin-Al_{13} polycation) and 0.9 × 1.2 × 2.0 nm^3 (Keggin-Al_{30} polycation) were considered for the models in **Figure 14**. Both these systems involve electrostatic interactions with the layers of the clay and are configured differently in this interlayer region. This difference in configuration explains why both Al-PILC differ in their surface area and in the number of micro- and mesopores (Wen et al., 2019b). The symmetrical structure of Al_{13} is similar to a sphere, therefore the surface charges are distributed evenly and arranged in the interlayer region in a nonspecific manner. The specific “flat-lying” arrangement of the Keggin-Al_{30} polycation in the

interlayer region of montmorillonite is a result of its extremely high positive charge and the charge distribution on its surface, with the highest density of positive charges being in the "belt" of the structure, as discussed in the "Acidity and Reactivity" section. This, in addition to its large size compared to Keggin-Al_{13}, results in a PILC with a larger porosity and a larger surface area (Wen et al., 2019a). In the second work, Wen et al. (2019a) studied the formation, transformation, and properties of Al-Keggin structures during the stages, including the hydrolysis stage, the intercalating stage, and the calcination stage, focusing on the Keggin-Al_{30} polycation. These authors used various characterization techniques, such as field-emission scanning electron microscopy, thermogravimetric analyses, and X-ray diffraction, and later published the schematic representation of **Figure 8** as shown in the "Al_{13} and Al_{30} Formation" section. They concluded that, during the formation of Keggin-Al_{30}, the excess of monomeric Al species at high temperature was an important factor, in agreement with other authors, as discussed in that section.

Experimentally, one important parameter during intercalation is the Al/clay ratio used, although the quantity of pillars intercalated depends on the charge of the pillars, the presence of other charged species in the solution, and the CEC of the clay (Cool and Vansant, 1998), as mentioned previously. Over the past few years, several authors have studied the implications of varying the aluminum/clay ratios (Gil and Montes, 1994a; Gil et al., 2007; Molina et al., 1992; Pesquera et al., 1991; Salerno et al., 2001; Stacey, 1988; Tokarz and Shabtai, 1985), and others have used Al/Clay (mmol/g) ratios of 2.0 (Maes et al., 1997; Shabtai et al., 1984), 3.0 (Butman et al., 2015), 4.0 (Matsuda et al., 1988; Matsuda et al., 1987; Wen et al., 2019a; Wen et al., 2019b; Zhu et al., 2018; Zhu et al., 2017), 5.0 (Gil et al., 2000b), 7.0 (Moreno et al., 1997), 10.0 (Cheng and Yang, 1997; Hutson et al., 1999), and 20.0 (Zuo and Zhou, 2008) in their studies. Gil et al. (2007), for example, used nitrogen and carbon dioxide adsorption methods to study the structural properties of Al-PILC montmorillonites obtained upon varying the Al/clay ratio (10, 30, 90, and 150 mmol/dm^3 Al^{III}/g clay) and calcination temperature (200, 400 and 500 °C). These authors reported that an increase in both the Al/clay ratio and treatment temperature

reduced the surface area and micropore volume of the clays. They also found that a lower Al/clay ratio (mmol/dm^3 Al^{III}/g clay) was sufficient to achieve successful intercalation.

For the intercalation of both Al_{13} and Al_{30} clusters into montmorillonite, two methods comprising the use of the clay mineral as a powder or use as an aqueous dispersion have been reported in the literature. However, PILC prepared using the clay mineral as a powder are much more affordable and produce highly porous, homogeneously intercalated clays (Cool and Vansant, 1998). Some of the parameters reported for each intercalation method and each polycation (Al_{13} and Al_{30}) are presented below. Thus, for the Al_{13} polycation, studies involving dropwise addition of the intercalating solution to an aqueous suspension (0.002 – 2.5%) of the montmorillonite with stirring (Bradley et al., 1990; Butman et al., 2015; Cheng and Yang, 1997; Gil and Montes, 1994a; Gil et al., 2007; Hutson et al., 1999; Lahav et al., 1978; Moreno et al., 1997; Pesquera et al., 1991; Plee et al., 1987; Salerno et al., 2001; Shabtai et al., 1984; Stacey, 1988; Suzuki et al., 1988; Tokarz and Shabtai, 1985; Zuo and Zhou, 2008), at room temperature for 12, 24, or 48 h (Cheng and Yang, 1997; Gil and Montes, 1994a, b; Gil et al., 2007; Hutson et al., 1999; Molina et al., 1992; Moreno et al., 1997; Suzuki et al., 1988), or, in some cases, at higher temperatures such as 60 °C for 3 h (Zuo and Zhou, 2008), or 80 °C for 2 h (Butman et al., 2015), have been reported. Some of these mixtures were aged for 12 h (Butman et al., 2015) or 24 h (Pesquera et al., 1991) after the addition had finished. When using montmorillonite as a powder, the addition thereof to intercalating solutions of Al_{13} with continuous stirring has been reported at room temperature for 24 h (Gil et al., 2000b), at 70 °C for 1 h (Matsuda et al., 1988; Matsuda et al., 1987), and at 60 °C for 24 h, and when using the latter method, the mixture was aged for 24 h at the same temperature (Wen et al., 2019a; Wen et al., 2019b; Zhu et al., 2018; Zhu et al., 2017). Various authors have explored alternatives to improve the synthesis method by making it a shorter and less tedious process. Thus, Fetter et al. (1996 and 1997) and Sampieri et al. (2004) compared the conventional intercalation process with the use of a version involving microwave irradiation and

found that the use thereof has advantages, such as making the pillaring process possible in less than 15 minutes, the elimination of organic impurities from the clay, and the possibility of using both concentrated aluminum solutions and clay suspensions in the intercalation process.

In the case of the Al_{30} polycation, the use of a 1 wt.% aqueous suspension of montmorillonite has been reported, adding the intercalating solution to it dropwise at 80 °C for 2 h, followed by aging for 12 h at room temperature (Butman et al., 2015). The dispersion of montmorillonite as a powder into the intercalating solutions of Al_{30} has been reported at 95 °C for 24 h, with an aging time of 24 h at the same temperature (Wen et al., 2019a; Wen et al., 2019b; Zhu et al., 2018; Zhu et al., 2017). In both cases, the procedures were carried out with continuous stirring.

8. Washing, drying, and calcination steps

The intercalation process is followed by the separation of the intercalated clay and the solution, which includes two important steps, namely washing and drying the intercalated clay. These steps precede the calcination required to obtain the pillared clay and both of them seem to improve the quality of the PILC. The washing step promotes an equal dispensation of pillars between the layers and forms larger interlayer spacings. Indeed, differences exist between the Al-PILC if they are unwashed (1.2 nm) or washed (1.8 nm) (Cool and Vansant, 1998), whereas the drying step can affect the pore size and its uniformity (Gil et al., 2008; Salerno et al., 2001). Cooling to room temperature is necessary in some cases. Both filtration (Cheng and Yang, 1997; Hutson et al., 1999; Matsuda et al., 1988; Matsuda et al., 1987; Wen et al., 2019a; Wen et al., 2019b; Zhu et al., 2018; Zhu et al., 2017; Zuo and Zhou, 2008), and centrifugation (Butman et al., 2015; Gil and Montes, 1994a, b; Gil et al., 2007; Gil et al., 2000b; Stacey, 1988; Suzuki et al., 1988; Tokarz and Shabtai, 1985) have been used in the separation process. In both cases, the washing process is repeated on the solid obtained, using distilled water to remove both chloride and excess interclating solution. Finally, to dry the samples, there are

reports of slow drying in an oven at temperatures of 50 – 60 °C (Butman et al., 2015; Gil et al., 2007; Gil et al., 2000b; Suzuki et al., 1988), 80 °C (Salerno et al., 2001), and 20 - 100 °C, (Gil and Montes, 1994a, b; Hutson et al., 1999; Matsuda et al., 1988; Matsuda et al., 1987; Stacey, 1988; Trillo et al., 1993; Zuo and Zhou, 2008), in some cases overnight. Quick-drying techniques such as freeze-drying have also been reported (Moreno et al., 1997; Pesquera et al., 1991; Plee et al., 1987; Tokarz and Shabtai, 1985; Wen et al., 2019a; Wen et al., 2019b; Zhu et al., 2018; Zhu et al., 2017). However, to obtain a well-ordered PILC, Trillo et al. (1993) recommended air-drying the sample instead of freeze-drying because the products obtained by freeze-drying showed meso- and macroporous structures. The use of air to dry the intercalated solids favors crystallinity and microporosity because this slow drying method allows the layers to fix themselves in a parallel and ordered manner (face-to-face stacking), whereas in quick drying methods, like freeze-drying, the aggregates form in a random manner (Cool and Vansant, 1998). The washing and drying steps are followed by calcination of the intercalated solid. This heating process is required to produce stable pillared clay. During this process, dehydration and dehydroxylation of the Al-polyoxocations occur, thus converting these precursors into neutral and rigid alumina oxide pillars (Casey, 2005; Cool and Vansant, 1998). The PILC obtained are permanently microporous and will not be affected by phenomena like expansion or hydrolysis, although the protons remaining in their interlayer regions remain candidates for ion exchange (Cool and Vansant, 1998).

The preceding sections noted that, among the experimental parameters that can be adjusted in the synthesis process to control the characteristics and microstructure in Al-PILC, the calcination step has shown to have a marked effect on the texture of the Al-PILC montmorillonites, as shown by Gil et al. (1994b, 2007, 2008). In this regard, Zhu et al. (2018) used techniques such as thermogravimetric analysis, N_2 adsorption-desorption, and high-temperature X-ray diffraction to compare the thermal stability of montmorillonites, both natural and pillared using both Al_{13}-, and Al_{30}-Keggin polycations. These authors found that both Al-PILC (Al_{13}

and Al_{30}) exhibit improved thermal stability, and proved that Al_{30}-PILC is the most thermally stable of them. Their results showed that while the layers of the natural clay collapsed at 200 °C, the layers of Al_{30}-PILC remained unchanged, even at a calcination temperature of 800 °C.

The Al_{30} cluster is more compact than the Al_{13} cluster due to the smaller O-Al-O bond angles and shorter η-OH_2 and μ-OH bond distances, thus giving it higher thermal stability. As a result, the Al_{30}-PILC montmorillonite structure is stable up to 800 °C (Wen et al., 2019a). The use of both Al_{13} and Al_{30} polycations in the pillaring process improves the thermal stability of montmorillonite due to the formation of Al oxides with high thermal stability as pillars in the interlayer region. This provides protection and allows retention of the layered structure as micro/mesoporous structures at high temperatures (Wen et al., 2019a; Zhu et al., 2018). In the calcination step, both Keggin polycations (Al_{13} and Al_{30}) lose water molecules as the temperature increases, the first being the η-OH_2 groups due to the relative weakness of the Al-OH_2 bond (Wen et al., 2019a).

Motalov et al. (2017) used mass spectrometry to compare the thermal emission of alkali metal ions (Li^+, Na^+, K^+, Rb^+, and Cs^+) in Al_{30}-pillared montmorillonite and its natural form (from 500 to 660 °C in both cases). These authors observed an emission anomaly in the temperature range 532 – 559 °C, which they assigned to the chemical transformations of the pillars and concurrent reactions with the alkali metal ions.

Al_{13}-pillared montmorillonites have been reported as having been obtained after calcination in a furnace at 300 °C for 2 – 3 h (Butman et al., 2015; Plee et al., 1987; Wen et al., 2019b; Zhu et al., 2017), 350 °C for 12 h (Cheng and Yang, 1997), 400 °C for 2 – 4 h (Maes et al., 1997; Matsuda et al., 1987; Molina et al., 1992), and 500 °C for 1 – 4 h (Gil et al., 2000b; Salerno et al., 2001; Suzuki et al., 1988; Suzuki and Mori, 1989; Zuo and Zhou, 2008). To obtain information about the thermal stability of these Al_{13}-PILC montmorillonites, and to study the effect of calcination

temperature on their textural properties, several studies have evaluated several calcination temperatures, such as 200 – 600 °C for 3 – 4 h (Gil and Montes, 1994b; Gil et al., 2007; Moreno et al., 1997; Pesquera et al., 1991; Stacey, 1988), 300 - 700 °C for 4 – 6 h (Matsuda et al., 1988; Trillo et al., 1993), 400 and 600 °C for 12 h (Hutson et al., 1999), and 200 – 1100 °C (Wen et al., 2019a; Zhu et al., 2018). Al_{30}-pillared montmorillonites can be obtained after calcination at 300 °C for 2 - 3 h (Butman et al., 2015; Wen et al., 2019a; Wen et al., 2019b; Zhu et al., 2017), 350 °C for 3 h (Motalov et al., 2017), at higher temperatures such as 800 °C (Wen et al., 2019a), and at 200 - 1100 °C (Zhu et al., 2018). Other authors, such as de Andrés et al. (de Andrés et al., 1999), have studied the use of microwave irradiation instead of the conventional calcination step in aluminum pillared montmorillonite synthesis. Samples obtained in this way were intermediate between the intercalated clays and the PILC obtained using the standard calcination treatment.

9. Conclusions

The results summarized in this review show the great interest that has existed over the years in understanding both formations, namely Al_{13} and Al_{30} polycations, and Al_{13}- and Al_{30}-PILC montmorillonites. Some of the studies discussed herein show the effect of total aluminum and aluminum monomer concentrations on the process for synthesizing intercalating solutions. The importance of the experimental parameters used in both synthetic processes mentioned (intercalating solution and Al-PILC) is reflected in the majority of the manuscripts related to Al-PILC in this review. The results clearly illustrate researchers' attempts to propose several conditions for these processes to achieve the successful synthesis of both Al-PILC using Al_{13} and Al_{30} polycations as intercalant solutions while guaranteeing reproducible characteristics in the solids obtained. Some authors have also proposed future challenges in this field, which are mainly related to producing Al-PILC with higher microporosity and larger interlayer spacings, thereby further expanding their role and development as catalysts and adsorbent materials.

From the results included in this work, there are still many interesting areas to be explored for applications of PILC materials. The porous structure can be designed, controlled, and adapted to desired applications as the selective adsorption of pollutants, the synthesis of more selective catalysts for wastewater applications, and the development of biocatalysts by the immobilization of enzymes and micro-organisms.

Declaration of Competing Interest

No

Acknowledgments: The authors are grateful for financial support from the Spanish Ministry of Economy, Industry and Competitiveness (AEI/MINECO) and the European Regional Development Fund (ERDF) through project MAT2016-78863-C2-R. YC thanks the Universidad Pública de Navarra for a pre-doctoral grant (IberusTalent, European Union's H2020 research and innovation programme under Marie Sklodowska-Curie grant agreement N° 801586). AG also thanks Santander Bank for funding via the Research Intensification Program.

References

Abeysinghe, S., Corum, K.W., Neff, D.L., Mason, S.E., Forbes, T.Z., 2013a. Contaminant adsorption on nanoscale particles: structural and theoretical characterization of Cu^{2+} bonding on the surface of Keggin-type polyaluminum (Al_{30}) molecular species. Langmuir. 29, 14124-14134.

Abeysinghe, S., Unruh, D.K., Forbes, T.Z., 2012. Crystallization of Keggin-type polyaluminum species by supramolecular interactions with disulfonate anions. Cryst. Growth Des. 12, 2044-2051.

Abeysinghe, S., Unruh, D.K., Forbes, T.Z., 2013b. Surface modification of Al_{30} Keggin-type polyaluminum molecular clusters. Inorg. Chem. 52, 5991-5999.

Akitt, J.W., Greenwood, N.N., Khandelwal, B.L., Lester, G.D., 1972. ^{27}Al nuclear magnetic resonance studies of the hydrolysis and polymerisation of the hexa-aquo-aluminium(III) cation. Dalton Trans. 5, 604-610.

Allouche, L., Gérardin, C., Loiseau, T., Férey, G., Taulelle, F., 2000. Al_{30}: A giant aluminum polycation. Angew. Chem. Int. Ed. 39, 511 - 514.

Allouche, L., Taulelle, F., 2003a. Conversion of Al_{13} Keggin ε into Al_{30}: A reaction controlled by aluminum monomers. Inorg. Chem. commun. 6, 1167-1170.

Allouche, L., Taulelle, F., 2003b. Fluorination of the ε-Keggin Al_{13} polycation. Chem. Commun. 16, 2084-2085.

André Ohlin, C., Rustad, J.R., Casey, W.H., 2014. The energetics of isomerisation in Keggin-series aluminate cations. Dalton Trans. 43, 14533-14536.

Baloyi, J., Ntho, T., Moma, J., 2018. Synthesis and application of pillared clay heterogeneous catalysts for wastewater treatment: a review. RSC Adv. 8, 5197-5211.

Bennett, J.W., Bjorklund, J.L., Forbes, T.Z., Mason, S.E., 2017. Systematic study of aluminum nanoclusters and anion adsorbates. Inorg. Chem. 56, 13014-13028.

Bottero, J.Y., Bersillon, J.L., 1988. Aluminum and iron(III) chemistry, aquatic humic substances. American Chemical Society, pp. 425-442.

Bottero, J.Y., Cases, J.M., Fiessinger, F., Poirier, J.E., 1980. Studies of hydrolyzed aluminum chloride solutions. 1. Nature of aluminum species and composition of aqueous solutions. J. Phys. Chem. 84, 2933-2939.

Bottero, J.Y., Tchoubar, D., Cases, J.M., Fiessinger, F., 1982. Investigation of the hydrolysis of aqueous solutions of aluminum chloride. 2. Nature and structure by small-angle x-ray scattering. J. Phys. Chem. 86, 3667-3673.

Bradley, S.M., Kydd, R.A., 1993. Ga_{13}, Al_{13}, $GaAl_{12}$, and Chromium-pillared montmorillonites: acidity and reactivity for cumene conversion. J. Catal. 141, 239-249.

Bradley, S.M., Kydd, R.A., Howe, R.F., 1993. The structure of Al gels formed through the base hydrolysis of Al^{3+} aqueous solutions. J. Colloid Interface Sci. 159, 405-412.

Bradley, S.M., Kydd, R.A., Yamdagni, R., 1990. Comparison of the hydrolyses of gallium(III) and aluminium(III) solutions by nuclear magnetic resonance spectroscopy. Dalton Trans. 9, 2653-2656.

Brosset, C., 1952. On the reactions of the aluminium ion with water. Acta Chem. Scand. 6, 910 - 940.

Brosset, C., Biedermann, G., Sillén, L.G., 1954. Studies on the hydrolysis of metal ions. XI. The Aluminium Ion, Al^{3+}. Acta Chem. Scand. 8, 1917 - 1926.

Butman, M.F., Belozerov, A.G., Karasev, N.S., Kochkina, N.E., Khodov, I.A., Ovchinnikov, N.L., 2015. Structural and textural properties of pillared montmorillonite at intercalation of large Al- and Al/Ce-polyhydroxocomplexes. Nanotechnol. Russ. 10, 706-712.

Cañizares, P., Valverde, J.L., Sun Kou, M.R., Molina, C.B., 1999. Synthesis and characterization of PILCs with single and mixed oxide pillars prepared from two different bentonites. A comparative study. Microporous Mesoporous Mater. 29, 267-281.

Casey, W., Olmstead, M., Fields, C., Lamar, C., Forbes, T., 2015. A new nanometer-sized Ga(III)-oxyhydroxide cation. Inorganics. 3, 21-26.

Casey, W.H., 2005. Large aqueous aluminum hydroxide molecules. Chem. Rev. 106, 1-16.

Casey, W.H., Olmstead, M.M., Phillips, B.L., 2005a. A new aluminum hydroxide octamer, $[Al_8(OH)_{14}(H_2O)_{18}](SO_4)_5 \cdot 16H_2O$. Inorg. Chem. 44, 4888-4890.

Casey, W.H., Phillips, B.L., Furrer, G., 2001. Aqueous aluminum polynuclear complexes and nanoclusters: a review. Rev. Mineral. Geochem. 44, 167-190.

Casey, W.H., Phillips, B.L., Karlsson, M., Nordin, S., Nordin, J.P., Sullivan, D.J., Neugebauer-Crawford, S., 2000. Rates and mechanisms of oxygen exchanges between sites in the $AlO_4Al_{12}(OH)_{24}(H_2O)_{12}^{7+}$(aq) complex and water: implications for mineral surface chemistry. Geochim. Cosmochim. Acta. 64, 2951-2964.

Casey, W.H., Rustad, J.R., Banerjee, D., Furrer, G., 2005b. Large molecules as models for small particles in aqueous geochemistry research. J. Nanopart. Res. 7, 377-387.

Clearfield, A., Roberts, B.D., 1988. Pillaring of layered zirconium and titanium phosphates. Inorg. Chem. 27, 3237-3240.

Cool, P., Vansant, E.F., 1998. Pillared clays: preparation, characterization and applications, synthesis. Molecular Sieves (Science and Technology). Springer Berlin Heidelberg, Berlin, Heidelberg, pp. 265-288.

Corum, K.W., Fairley, M., Unruh, D.K., Payne, M.K., Forbes, T.Z., Mason, S.E., 2015. Characterization of phosphate and arsenate adsorption onto Keggin-Type Al_{30} cations by experimental and theoretical methods. Inorg. Chem. 54, 8367-8374.

Chen, Z., Fan, B., Peng, X., Zhang, Z., Fan, J., Luan, Z., 2006. Evaluation of Al_{30} polynuclear species in polyaluminum solutions as coagulant for water treatment. Chemosphere. 64, 912-918.

Chen, Z., Liu, C., Luan, Z., Zhang, Z., Li, Y., Jia, Z., 2005. Effect of total aluminum concentration on the formation and transformation of nanosized Al_{13} and Al_{30} in hydrolytic polymeric aluminum aqueous solutions. Chinese Sci. Bull. 50, 2010-2015.

Chen, Z., Luan, Z., Fan, J., Zhang, Z., Peng, X., Fan, B., 2007. Effect of thermal treatment on the formation and transformation of Keggin Al_{13} and Al_{30} species in hydrolytic polymeric aluminum solutions. Colloids Surf. A Physicochem. Eng. Asp. 292, 110-118.

Chen, Z., Luan, Z., Jia, Z., Li, X., 2009. Study on the hydrolysis/precipitation behavior of Keggin Al_{13} and Al_{30} polymers in polyaluminum solutions. J. Environ. Manage. 90, 2831-2840.

Cheng, L.S., Yang, R.T., 1997. Tailoring micropore dimensions in pillared clays for enhanced gas adsorption. Microporous Materials. 8, 177-186.

de Andrés, A.M., Merino, J., Galván, J.C., Ruiz-Hitzky, E., 1999. Synthesis of pillared clays assisted by microwaves. Mater. Res. Bull. 34, 641-651.

Ding, M., Zuo, S., Qi, C., 2015. Preparation and characterization of novel composite AlCr-pillared clays and preliminary investigation for benzene adsorption. Appl. Clay. Sci. 115, 9-16.

Ding, Z., Kloprogge, J.T., Frost, R.L., Lu, G.Q., Zhu, H.Y.J.J.o.P.M., 2001. Porous clays and pillared clays-based catalysts. Part 2: a review of the catalytic and molecular sieve applications. J. Porous Mater. 8, 273-293.

Drljaca, A., J. Hardie, M., L. Raston, C., 1999. Selective isolation of Keggin ions using self-assembled superanion capsules†. Dalton Trans. 20, 3639-3642.

Fairley, M., Unruh, D.K., Abeysinghe, S., Forbes, T.Z., 2012. Synthesis and structural characterization of heterometallic thorium aluminum polynuclear molecular clusters. Inorg. Chem. 51, 9491-9498.

Feng, C., Wei, Q., Wang, S., Shi, B., Tang, H., 2007. Speciation of hydroxyl-Al polymers formed through simultaneous hydrolysis of aluminum salts and urea. Colloids Surf. A Physicochem. Eng. Asp. 303, 241-248.

Fetter, G., Heredia, G., Maubert, A.M., Bosch, P., 1996. Synthesis of Al-intercalated montmorillonites using microwave irradiation. J. Mater. Chem. 6, 1857-1858.

Fetter, G., Heredia, G., Velázquez, L.A., Maubert, A.M., Bosch, P., 1997. Synthesis of aluminum-pillared montmorillonites using highly concentrated clay suspensions. Appl. Catal. A Gen. 162, 41-45.

Fu, G., Nazar, L.F., Bain, A.D., 1991. Aging processes of alumina sol-gels: characterization of new aluminum polyoxycations by aluminum-^{27} NMR spectroscopy. Chem. Mater. 3, 602-610.

Furrer, G., Trusch, B., Müller, C., 1992. The formation of polynuclear Al_{13} under simulated natural conditions. Geochim. Cosmochim. Acta. 56, 3831-3838.

Galeano, L.-A., Vicente, M.Á., Gil, A., 2014. Catalytic degradation of organic pollutants in aqueous streams by mixed Al/M-pillared clays (M = Fe, Cu, Mn). Catal. Rev. Sci. Eng. 56, 239-287.

Gil, A., Assis, F.C.C., Albeniz, S., Korili, S.A., 2011a. Removal of dyes from wastewaters by adsorption on pillared clays. Chem. Eng. J. 168, 1032-1040.

Gil, A., Gandía, L.M., Vicente, M.A., 2000a. Recent advances in the synthesis and catalytic applications of pillared clays. Catal. Rev. Sci. Eng. 42, 145-212.

Gil, A., Korili, S., Trujillano, R., Vicente, M.A., 2011b. A review on characterization of pillared clays by specific techniques. Appl. Clay. Sci. 53, 97-105.
Gil, A., Korili, S.A., Trujillano, R., Vicente, M.A., 2011c. A review on characterization of pillared clays by specific techniques. Appl. Clay. Sci. 53, 97-105.
Gil, A., Korili, S.A., Vicente, M.A., 2008. Recent advances in the control and characterization of the porous structure of pillared clay catalysts. Catal. Rev. Sci. Eng. 50, 153-221.
Gil, A., Montes, M., 1994a. Analysis of the microporosity in pillared clays. Langmuir. 10, 291-297.
Gil, A., Montes, M., 1994b. Effect of thermal treatment on microporous accessibility in aluminium pillared clays. J. Mater. Chem. 4, 1491-1496.
Gil, A., Montes, M., 1994c. Evolution of the microporous accessibility with the hydrolysis degree and the intercalation solution ageing time conditions in aluminium-pillared clays. Microporous Mater. 3, 319-329.
Gil, A., Trujillano, R., Vicente, M.A., Korili, S.A., 2007. Analysis of the structure of alumina-pillared clays by nitrogen and carbon dioxide adsorption. Ads.Sci.Technol. 25, 217-226.
Gil, A., Vicente, M.A., 2020. Progress and perspectives on pillared clays applied in energetic and environmental remediation processes. Curr. Opin. Green Sustain. Chem. 21, 56-63.
Gil, A., Vicente, M.A., Gandía, L.M., 2000b. Main factors controlling the texture of zirconia and alumina pillared clays. Microporous Mesoporous Mater. 34, 115-125.
Guerra, D.L., Airoldi, C., Lemos, V.P., Angélica, R.S., 2008. Adsorptive, thermodynamic and kinetic performances of Al/Ti and Al/Zr-pillared clays from the Brazilian Amazon region for zinc cation removal. J. Hazard. Mater. 155, 230-242.
Hutson, N.D., Hoekstra, M.J., Yang, R.T., 1999. Control of microporosity of Al_2O_3-pillared clays: effect of pH, calcination temperature and clay cation exchange capacity. Microporous Mesoporous Mater. 28, 447-459.
Jlassi, K., Krupa, I., Chehimi, M.M., 2017. Chapter 1 - Overview: clay preparation, properties, modification, in: Jlassi, K., Chehimi, M.M., Thomas, S. (Eds.), Clay-Polymer Nanocomposites. Elsevier, pp. 1-28.
Johansson, G., 1960. On the crystal structures of some basic aluminium salts. Acta Chem. Scand. 14, 771 - 773.
Johansson, G., Lundgren, G., Sillén, L.G., Soderquist, R., 1960. On the crystal structure of a basic aluminium sulfate and the corresponding selenate. Acta Chem. Scand. 14, 769 - 771.
Jones, J.R., Purnell, J.H., 1993. Synthesis and characterisation of alumina pillared Texas montmorillonite and determination of the effective Keggin ion charge. Catal. Letters. 18, 137-140.
Kausar, A., Iqbal, M., Javed, A., Aftab, K., Nazli, Z.-i.-H., Bhatti, H.N., Nouren, S., 2018. Dyes adsorption using clay and modified clay: a review. J. Mol. Liq. 256, 395-407.
Kloprogge, J.T., Duong, L.V., Frost, R.L.J.E.G., 2005. A review of the synthesis and characterisation of pillared clays and related porous materials for cracking of vegetable oils to produce biofuels. Environ. Geol. 47, 967-981.
Kloprogge, J.T.J.J.o.P.M., 1998. Synthesis of smectites and porous pillared clay catalysts: a review. J. Porous Mater. 5, 5-41.
Kudynska, J., Buckmaster, H.A., Kawano, K., Bradley, S.M., Kydd, R.A., 1993. A 9 GHz cw-electron-paramagnetic resonance study of the sulphate salts of tridecameric $[Mn_xAl_{13-x}O_4(OH)_{24}(H_2O)_{12}]^{(7-x)+}$. J. Chem. Phys. 99, 3329-3334.
Lahav, N., Shani, U., Shabtai, J.J.C., Minerals, C., 1978. Cross-linked smectites. I. Synthesis and properties of hydroxy-aluminum-montmorillonite. Clays Clay Miner. 26, 107-115.
Lambert, J.F., Poncelet, G., 1997. Acidity in pillared clays: origin and catalytic manifestations. Topics in Catalysis 4, 43-56.
Lazaratou, C.V., Vayenas, D.V., Papoulis, D., 2020. The role of clays, clay minerals and clay-based materials for nitrate removal from water systems: a review. Appl. Clay. Sci. 185, 105377.
Lee, A.P., Phillips, B.L., Olmstead, M.M., Casey, W.H., 2001. Synthesis and characterization of the $GeO_4Al_{12}(OH)_{24}(OH_2)_{12}^{8+}$ polyoxocation. Inorg. Chem. 40, 4485-4487.
Maes, N., Heylen, I., Cool, P., Vansant, E.F., 1997. The relation between the synthesis of pillared clays and their resulting porosity. Appl. Clay. Sci. 12, 43-60.
Mainicheva, E.A., Gerasko, O.A., Sheludyakova, L.A., Naumov, D.Y., Naumova, M.I., Fedin, V.P., 2006. Synthesis and crystal structures of supramolecular compounds of polynuclear aluminum(III) aqua hydroxo complexes with cucurbit[6]uril. Russ. Chem. Bull. 55, 267-275.

Matsuda, T., Asanuma, M., Kikuchi, E., 1988. Effect of high-temperature treatment on the activity of montmorillonite pillared by alumina in the conversion of 1,2,4-trimethylbenzene. Appl. Catal. 38, 289-299.
Matsuda, T., Fuse, T., Kikuchi, E., 1987. The effect of spilled-over hydrogen on the activity of montmorillonite pillared by aluminum oxide for conversion of trimethylbenzenes. J. Catal. 106, 38-46.
Mensinger, Z.L., Gatlin, J.T., Meyers, S.T., Zakharov, L.N., Keszler, D.A., Johnson, D.W., 2008. Synthesis of heterometallic group 13 nanoclusters and inks for oxide thin-film transistors. Angew. Chem. Int. Ed. 47, 9484-9486.
Mertens, J., 2011. Al nanoclusters in coagulants and granulates: application in arsenic removal from water. Rev. Environ. Sci. Biotechnol. 10, 111-117.
Mertens, J., Casentini, B., Masion, A., Pothig, R., Wehrli, B., Furrer, G., 2012. Polyaluminum chloride with high Al_{30} content as removal agent for arsenic-contaminated well water. Water Res. 46, 53-62.
Mertens, J., Rose, J., Wehrli, B., Furrer, G., 2016. Arsenate uptake by Al nanoclusters and other Al-based sorbents during water treatment. Water Res. 88, 844-851.
Mesmer, R.E., Baes, C.F., 1990. Review of hydrolysis behavior of ions in aqueous solutions. MRS Proceedings. 180, 85.
Mokaya, R., Jones, W., 1993. Pillared acid-activated clays: synthesis, characterisation and application to chlorophyll adsorption, in: Sequeira, C.A.C., Hudson, M.J. (Eds.), Multifunctional Mesoporous Inorganic Solids. Springer Netherlands, Dordrecht, pp. 425-432.
Molina, R., Vieira-Coelho, A., Poncelet, G., 1992. Hydroxy-Al pillaring of concentrated clay suspensions. Clays Clay Miner. 40, 480-482.
Moreno, S., Sun Kou, R., Poncelet, G., 1997. Influence of preparation variables on the structural, textural, and catalytic properties of Al-pillared smectites. J. Phys. Chem. B. 101, 1569-1578.
Motalov, V., Karasev, N., Ovchinnikov, N., Butman, M., 2017. Thermal emission of alkali metal ions from Al_{30}-pillared montmorillonite studied by mass spectrometric method. J Anal. Methods. Chem. 2017, 1-6.
Muñoz, H.-J., Blanco, C., Gil, A., Vicente, M.-Á., Galeano, L.-A., 2017. Preparation of Al/Fe-pillared clays: effect of the starting mineral. Materials. 10, 1364.
Nazar, L.F., Fu, G., Bain, A.D., 1992. ^{27}Al MAS NMR studies of a new polyoxyaluminium cluster and its selective transformation to five-coordinate aluminium in the solid state. J. Chem. Soc., Chem. Commun. 3, 251-253.
Ngulube, T., Gumbo, J.R., Masindi, V., Maity, A., 2017. An update on synthetic dyes adsorption onto clay based minerals: A state-of-art review. J. Environ. Manage. 191, 35-57.
Nunes, C.D., Pires, J., Carvalho, A.P., Calhorda, M.J., Ferreira, P., 2008. Synthesis and characterisation of organo-silica hydrophobic clay heterostructures for volatile organic compounds removal. Microporous Mesoporous Mater. 111, 612-619.
Oliveri, A.F., Colla, C.A., Perkins, C.K., Akhavantabib, N., Callahan, J.R., Pilgrim, C.D., Smart, S.E., Cheong, P.H.-Y., Pan, L., Casey, W.H., 2016. Isomerization of Keggin Al_{13} ions followed by diffusion rates. Chem. Eur. J. 22, 18637-18637.
Osorio-Revilla, G., Gallardo-Velazquez, T., Cortez, M.D.S., Arellano, S., 2006. Immersion drying of wheat using Al-PILC, zeolite, clay, and sand as particulate media. Dry. Technol. 24, 1033-1038.
Oszkó, A., Kiss, J., Kiricsi, I., 1999. XPS investigations on the feasibility of isomorphous substitution of octahedral Al^{3+} for Fe^{3+} in Keggin ion salts. Phys. Chem. Chem. Phys. 1, 2565-2568.
Parker, W.O., Jr., Millini, R., Kiricsi, I., 1997. Metal substitution in Keggin-type tridecameric aluminum-oxo-hydroxy clusters. Inorg. Chem. 36, 571-575.
Pesquera, C., Gonzalez, F., Benito, I., Mendioroz, S., Pajares, J.A., 1991. Synthesis and characterization of pillared montmorillonite catalysts. Appl. Catal. 69, 97-104.
Phillips, B.L., Lee, A., Casey, W.H., 2003. Rates of oxygen exchange between the $Al_2O_8Al_{28}(OH)_{56}(H_2O)_{26}^{18+}$(aq) ($Al_{30}$) molecule and aqueous solution. Geochim. Cosmochim. Acta. 67, 2725-2733.
Phillips, B.L., Vaughn, J.S., Smart, S., Pan, L., 2016. Characterization of Al_{30} in commercial poly-aluminum chlorohydrate by solid-state ^{27}Al NMR spectroscopy. J. Colloid Interface Sci. 476, 230-239.

Pinnavaia, T.J., Tzou, M.-S., Landau, S.D., Raythatha, R.H., 1984. On the pillaring and delamination of smectite clay catalysts by polyoxo cations of aluminum. J. Mol. Catal. 27, 195-212.
Plee, D., Gatineau, L., Fripiat, J.J., 1987. Pillaring processes of smectites with and without tetrahedral substitution. Clays Clay Miner. 35, 81-88.
Polubesova, T., Undabeytia, T., Nir, S., Chertkova, L., Van Damme, H., Annabi-Bergaya, F., 2000. Adsorption of sulfometuron and other anions on pillared clay. J. Environ. Qual. 29, 948-954.
Rakotonarivo, E., Bottero, J.Y., Oases, J.M., Fiessinger, F., 1984. Study of the adsorption of long chain alkylsulfonates from aqueous solutions on aluminum hydroxide gels. Colloids Surf. 9, 273-292.
Rowsell, J., Nazar, L.F., 2000. Speciation and thermal transformation in alumina sols: structures of the polyhydroxyoxoaluminum cluster $[Al_{30}O_8(OH)_{56}(H_2O)_{26}]^{18+}$ and its δ-keggin moieté. J. Am. Chem. Soc. 122, 3777-3778.
Rustad, J., 2005. Molecular dynamics simulation of the titration of polyoxocations in aqueous solution. Geochim. Cosmochim. Acta. 69, 4397-4410.
Salerno, P., Asenjo, M.B., Mendioroz, S., 2001. Influence of preparation method on thermal stability and acidity of Al–PILCs. Thermochim. Acta. 379, 101-109.
Sampieri, A., Fetter, G., Bosch, P., Bulbulian, S., 2004. Washing effect on the synthesis of silica-pillared clays. J. Porous Mater. 11, 157-162.
Shabtai, J., Rosell, M., Tokarz, M., 1984. Cross-linked smectites. III. Synthesis and properties of hydroxy-aluminum hectorites and fluorhectorites. Clays Clay Miner. 32, 99-107.
Shafran, K., Deschaume, O., Perry, C.C., 2004. High-temperature speciation studies of Al-ion hydrolysis. Adv. Eng. Mater. 6, 836-839.
Shafran, K.L., Perry, C.C., 2005. A systematic investigation of aluminium ion speciation at high temperature. Part 1. Solution studies. Dalton Trans. (Cambridge, England : 2003), 2098-2105.
Sillén, L.G., 1954. On equilibria in systems with polynuclear complex formation. I. Methods for deducing the composition of the complexes from experimental data. "Core + Links" complexes. Acta Chem. Scand. 8, 299 - 317.
Sivaiah, M.V., Petit, S., Brendlé, J., Patrier, P., 2010. Rapid synthesis of aluminium polycations by microwave assisted hydrolysis of aluminium via decomposition of urea and preparation of Al-pillared montmorillonite. Appl. Clay. Sci. 48, 138-145.
Smart, S.E., Vaughn, J., Pappas, I., Pan, L., 2013. Controlled step-wise isomerization of the Keggin-type Al_{13} and determination of the γ-Al_{13} structure. Chem. Commun. 49, 11352-11354.
Stacey, M.H., 1988. Alumina-pillared clays and their adsorptive properties. Catal. Today. 2, 621-631.
Sterte, J., 1988. Hydrothermal treatment of hydroxycation precursor solutions. Catal. Today. 2, 219-231.
Sterte, J., Otterstedt, J.E., Thulin, H., Massoth, F.E., 1988. Characterization of alumina-montmorillonite complexes. Appl. Catal. 38, 119-129.
Sterte, J.P., Otterstedt, J.E., 1987. Aluminum-oxide-pillared montmorillonite: effect of hydrothermal treatment of pillaring solution on the product structure, in: Delmon, B., Grange, P., Jacobs, P.A., Poncelet, G. (Eds.), Studies in Surface Science and Catalysis. Elsevier, pp. 631-648.
Sun, Z., Wang, H., Tong, H., Sun, S., 2011. A giant polyaluminum species S-Al_{32} and two aluminum polyoxocations involving coordination by sulfate ions S-Al_{32} and S-K-Al_{13}. Inorg. Chem. 50, 559-564.
Suzuki, K., Horio, M., Mori, T., 1988. Preparation of alumina-pillared montmorillonite with desired pillar population. Mater. Res. Bull. 23, 1711-1718.
Suzuki, K., Mori, T., 1989. Synthesis of alumina-pillared clay with desired pillar population using Na-montmorillonite having controlled cation exchage capacity. J. Chem. Soc., Chem. Commun. 1, 7-8.
Tokarz, M., Shabtai, J., 1985. Cross-linked smectites. IV. Preparation and properties of hydroxyaluminum-pillared Ce- and La-montmorillonites and fluorinated NH_4^+-montmorillonites. Clays Clay Miner. 33, 89-98.
Trillo, J.M., Alba, M.D., Castro, M.A., Poyato, J., Tobías, M.M., 1993. Alumina-pillared montmorillonite: effect of thermal and hydrothermal treatment on the accessible micropore volume. J. Mater. Sci. 28, 373-378.
Vaughan, D.E.W., 1988. Pillared clays - a historical perspective. Catal. Today. 2, 187-198.

Vicente, M.A., Gil, A., Bergaya, F., 2013. Chapter 10.5 - Pillared clays clay miner., in: Bergaya, F., Lagaly, G. (Eds.), Developments in Clay Science. Elsevier, pp. 523-557.
Vogels, R.J.M.J., Kloprogge, J.T., Geus, J.W., 2005. Homogeneous forced hydrolysis of aluminum through the thermal decomposition of urea. J. Colloid Interface Sci. 285, 86-93.
Wang, W., Wentz, K.M., Hayes, S.E., Johnson, D.W., Keszler, D.A., 2011. Synthesis of the hydroxide cluster $[Al_{13}(\mu_3\text{-}OH)_6(\mu\text{-}OH)_{18}(H_2O)_{24}]^{15+}$ from an aqueous solution. Inorg. Chem. 50, 4683-4685.
Wehrli, B., Wieland, E., Furrer, G., 1990. Chemical mechanisms in the dissolution kinetics of minerals; the aspect of active sites. Aquat. Sci. 52, 3-31.
Wen, K., Wei, J., He, H., Zhu, J., Xi, Y., 2019a. Keggin-Al_{30}: An intercalant for keggin-Al_{30} pillared montmorillonite. Appl. Clay. Sci. 180, 105203.
Wen, K., Zhu, J., Chen, H., Ma, L., Liu, H., Zhu, R., Xi, Y., He, H., 2019b. Arrangement models of keggin-Al_{30} and keggin-Al_{13} in the interlayer of montmorillonite and the impacts of pillaring on surface acidity: a comparative study on catalytic oxidation of toluene. Langmuir. 35, 382-390.
Wood, T.E., Siedle, A.R., Hill, J.R., Skarjune, R.P., Goodbrake, C.J., 1990. Hydrolysis of aluminum-are all gels created equal?. MRS Proceedings. 180, 97.
Wu, Z., Zhang, X., Zhou, C., Pang, J., Zhang, P., 2016. A comparative study on the characteristics and coagulation mechanism of PAC-Al_{13} and PAC-Al_{30}. RSC Adv. 6, 108369-108374.
Ye, C., Bi, Z., Wang, D., 2013. Formation of Al_{30} from aqueous polyaluminum chloride under high temperature: Role of Al_{13} aggregates. Colloids Surf. A Physicochem. Eng. Asp. 436, 782-786.
Yuan, P., Yin, X., He, H., Yang, D., Wang, L., Zhu, J., 2006. Investigation on the delaminated-pillared structure of TiO_2-PILC synthesized by $TiCl_4$ hydrolysis method. Microporous Mesoporous Mater. 93, 240-247.
Zhu, J., Wen, K., Wang, Y., Ma, L., Su, X., Zhu, R., Xi, Y., He, H., 2018. Superior thermal stability of Keggin-Al_{30} pillared montmorillonite: A comparative study with Keggin-Al_{13} pillared montmorillonite. Microporous Mesoporous Mater. 265, 104-111.
Zhu, J., Wen, K., Zhang, P., Wang, Y., Ma, L., Xi, Y., Zhu, R., Liu, H., He, H., 2017. Keggin-Al_{30} pillared montmorillonite. Microporous Mesoporous Mater. 242, 256-263.
Zuo, S., Liu, F., Zhou, R., Qi, C., 2012. Adsorption/desorption and catalytic oxidation of VOCs on montmorillonite and pillared clays. Catal. Commun. 22, 1-5.
Zuo, S., Zhou, R., 2008. Influence of synthesis condition on pore structure of Al pillared clays and supported Pd catalysts for deep oxidation of benzene. Microporous Mesoporous Mater. 113, 472-480.

CAPTIONS

Figure 1. Schematic structure of the TOT montmorillonite (Reproduced with permission from Liu and Zhang, 2014).

Figure 2. (a) Comparison of the hydration and dehydration behavior of a natural clay mineral and a pillared clay. **(b)** Pillaring process (Reproduced with permission from Cool and Vansant, 1998).

Figure 3. The distribution curve of the different Al^{III} species present in the $AlCl_3$ solution hydrolyzed with NaOH, depending on the pH and OH/Al ratio. Published by Cool and Vansant (Reproduced with permission from Cool and Vansant, 1998), corresponding to the NMR and potentiometric titration results published by Bottero et al. (Reproduced with permission from Bottero et al, 1980, 1982).

Figure 4. Polyhedral representation: **(a)** Al_{13}; **(b)** AlP_1, **(c)** a possible "unsaturated" structure for AlP_2, **(d)** a "saturated" structure for AlP_2 (Reproduced with permission from Fu et al, 1991).

Figure 5. Proposed formation of Al_{30} initiated by aluminum monomers with ε-Al_{13} as precursor species (Reproduced with permission from Allouche and Taulelle, 2003).

Figure 6. Al-ion hydrolysis speciation diagram at 90 °C (Reproduced with permission from Shafran et al., 2004).

Figure 7. The formation mechanism of the large polymeric species Al_{26}, Al_{30}, and Al_{32}S (Reproduced with permission from Abeysinghe et al, 2012).

Figure 8. The formation process of the polycations Keggin-Al_{13} **(a)** and Keggin-Al_{30} **(b)** (Reproduced with permission from Wen et al, 2019a).

Figure 9. Surface functional groups: **(a, c)** Bound water molecules (η-H_2O) in Al_{13} and Al_{30}, respectively; **(b, d)** bridging hydroxide ions in Al_{13} and Al_{30} respectively (Reproduced with permission from Rustad, 2005).

Figure 10. (a) The surface charge density of Al_{30}^{16+} (Reproduced with permission from Abeysinghe et al, 2013). **(b)** Outer-sphere water molecule (top) and anion (bottom) distribution around an Al_{30} molecule in the skeletal form (Reproduced with permission from Casey et al., 2005).

Figure 11. Representation of the synthesis of Al_{30} **(a)** and Al_{30}-PILC montmorillonite **(b)** (Reproduced with permission from Zhu et al., 2017).

Figure 12. Pillared Interlayered Clays: general preparation procedure.

Figure 13. Possible acid sites in the montmorillonite (Reproduced with permission from Wen et al, 2019b).

Figure 14. Al-polycation arrangement models in montmorillonite. Top view of Keggin polycations Al_{13} **(A)** and Al_{30} **(B)**, and three-dimensional view of Keggin polycations Al_{13} **(C)** and Al_{30} **(D)** (Reproduced with permission from Wen et al, 2019b).

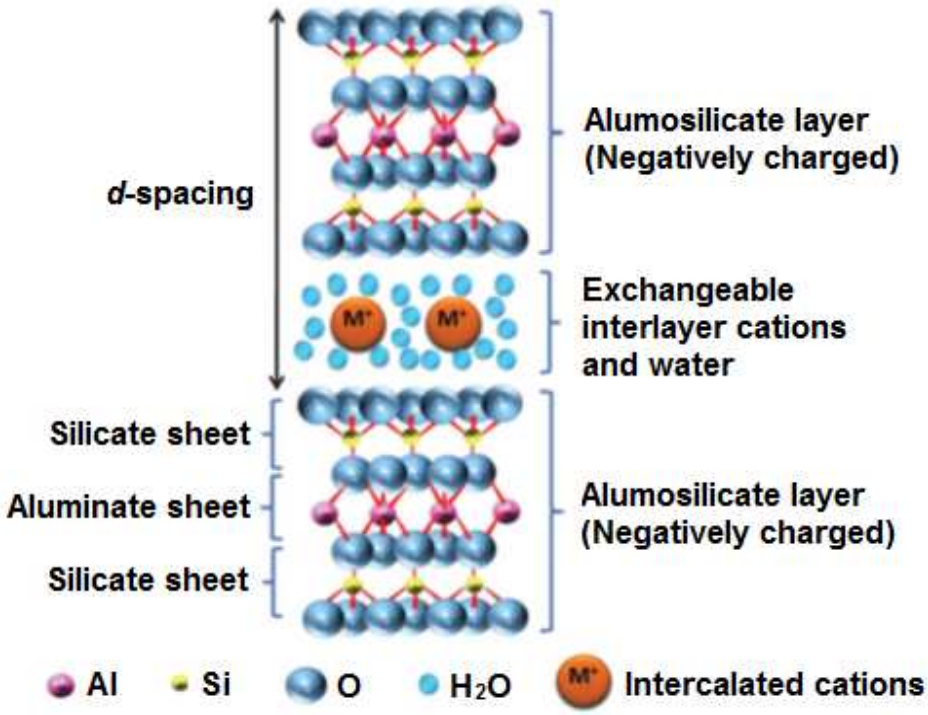

Figure 1. Schematic structure of the TOT montmorillonite (Reproduced with permission from Liu and Zhang, 2014).

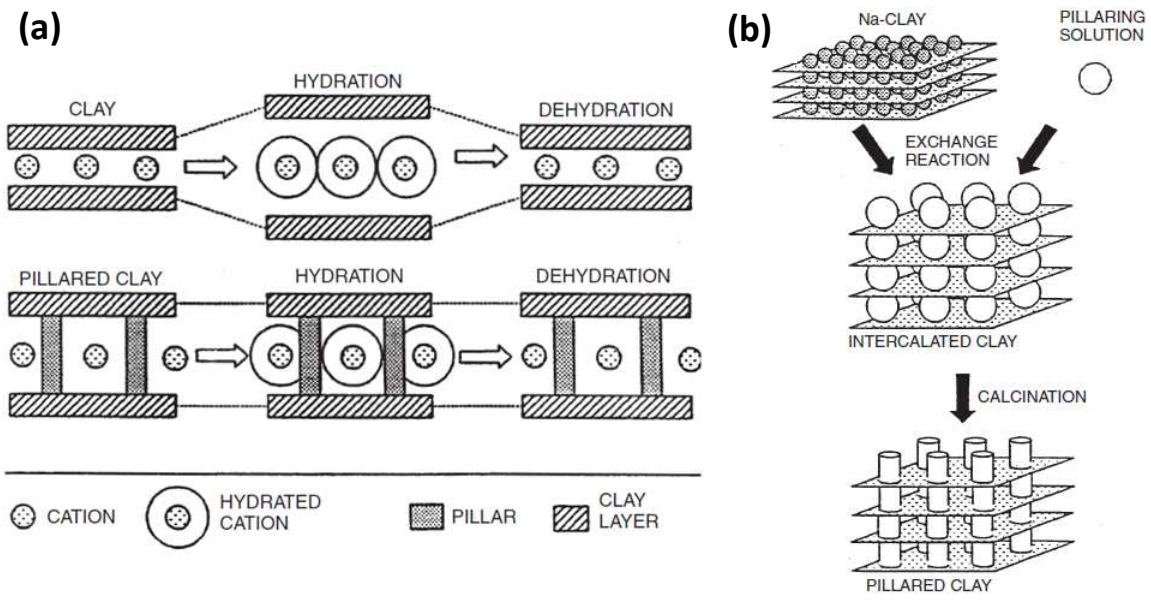

Figure 2. (a) Comparison of the hydration and dehydration behavior of a natural clay and a pillared clay. **(b)** Pillaring process (Reproduced with permission from Cool and Vansant, 1998).

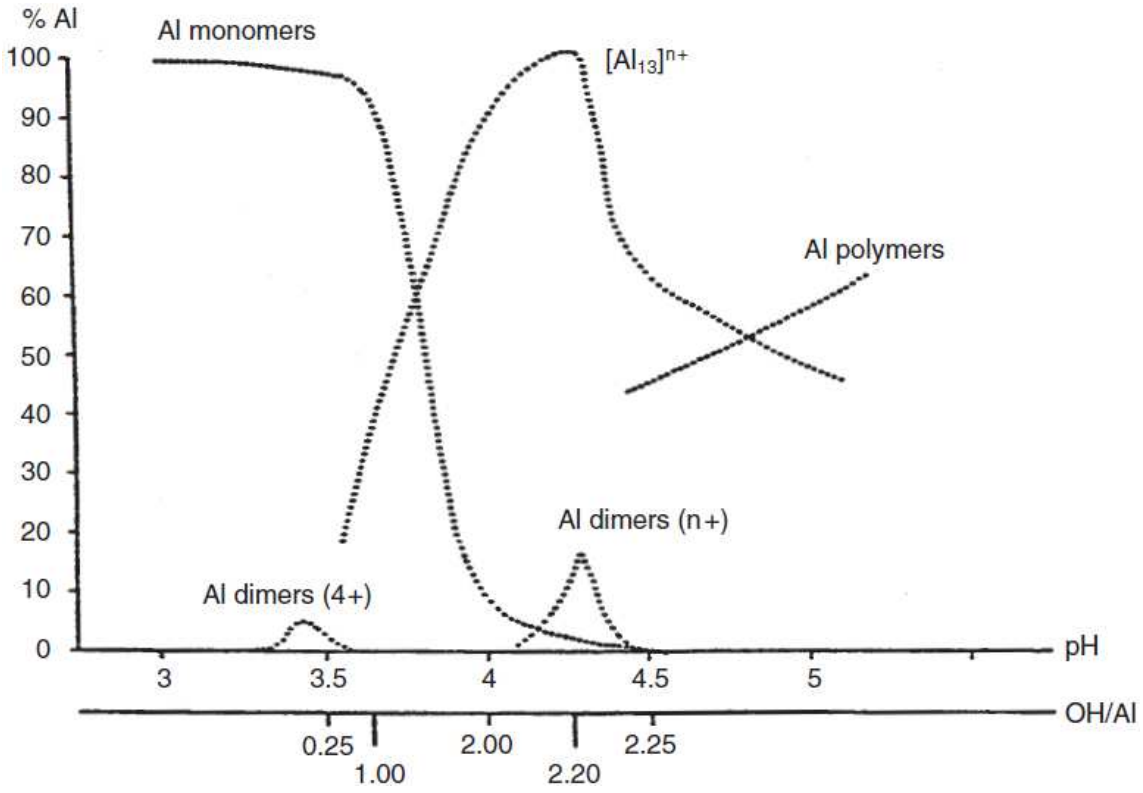

Figure 3. Distribution curve of the different Al^{III} species present in the $AlCl_3$ solution hydrolyzed with NaOH, depending on the pH and OH/Al ratio. Published by Cool and Vansant (Reproduced with permission from Cool and Vansant, 1998), corresponding to the NMR and potentiometric titration results published by Bottero et al. (Reproduced with permission from Bottero et al, 1980, 1982).

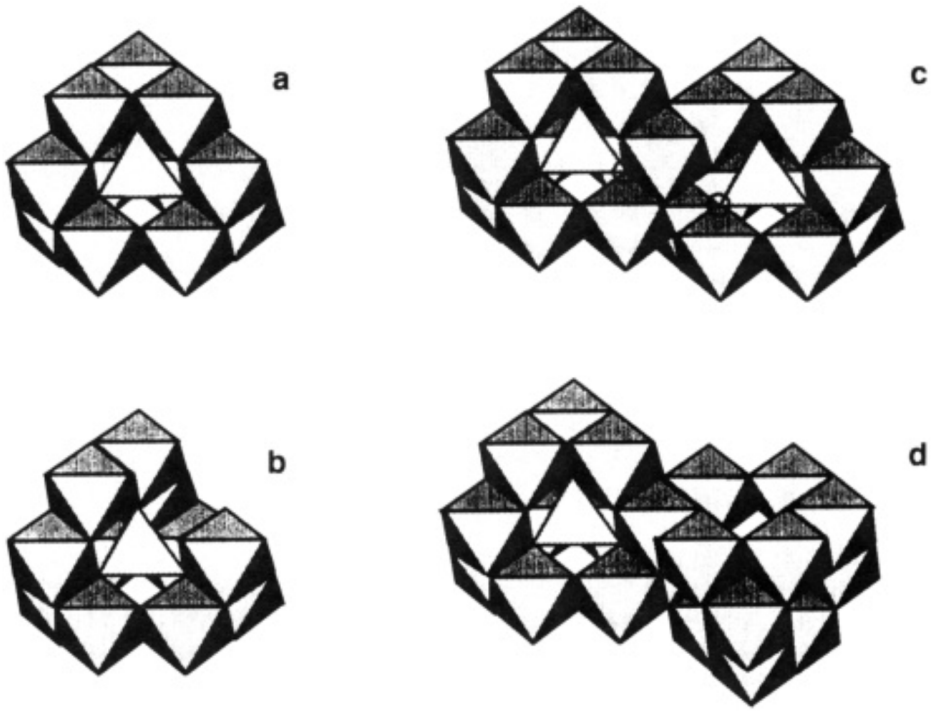

Figure 4. Polyhedral representation: **(a)** Al_{13}; **(b)** AlP_1, **(c)** a possible “unsaturated” structure for AlP_2, **(d)** a “saturated” structure for AlP_2 (Reproduced with permission from Fu et al, 1991).

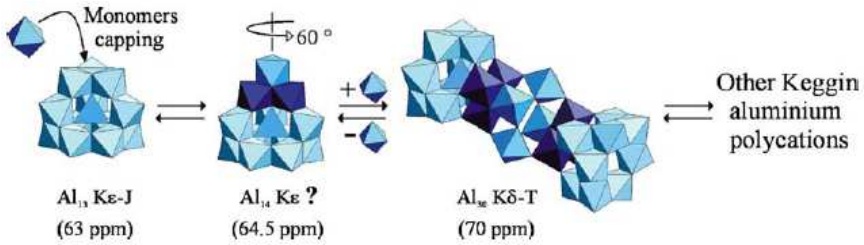

Figure 5. Proposed formation of Al_{30} initiated by aluminum monomers with ε-Al_{13} as precursor species (Reproduced with permission from Allouche and Taulelle, 2003).

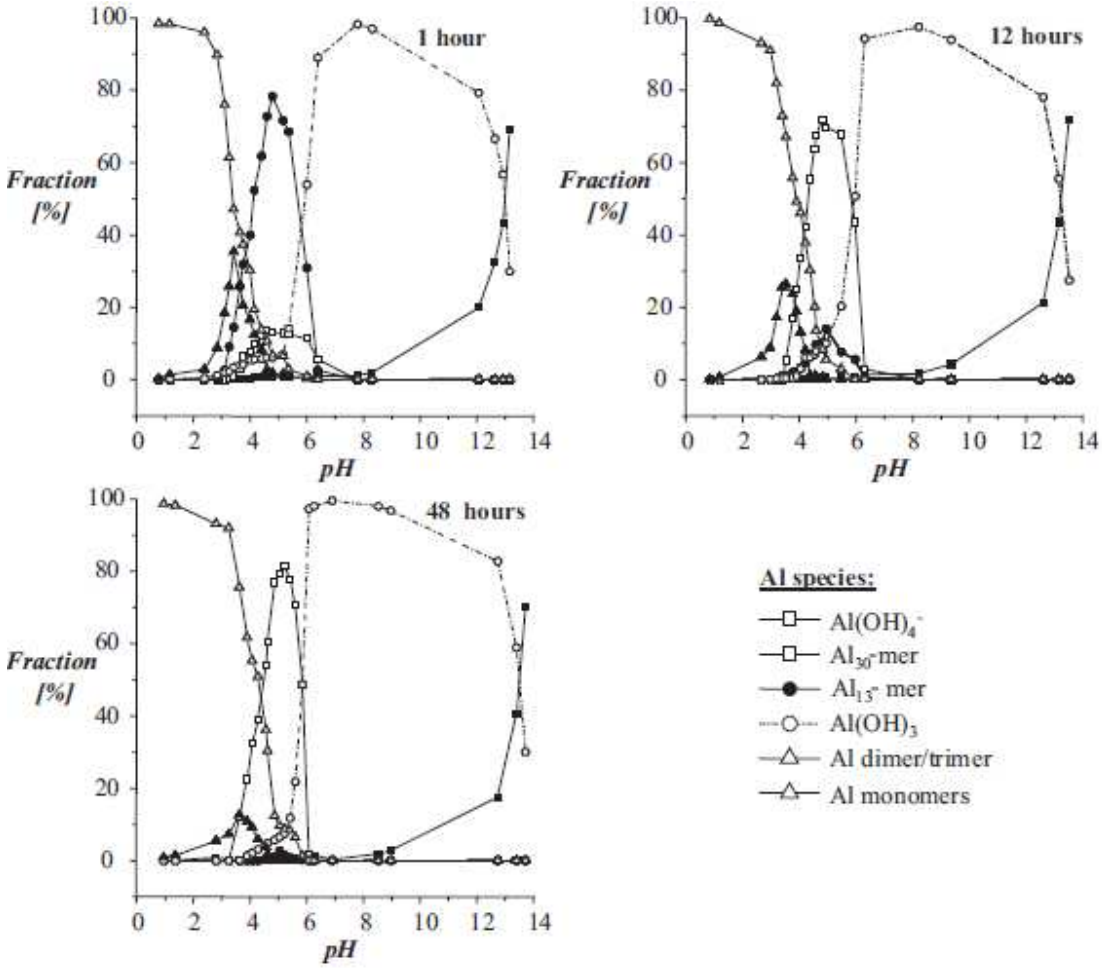

Figure 6. Al-ion hydrolysis speciation diagram at 90 °C (Reproduced with permission from Shafran et al., 2004).

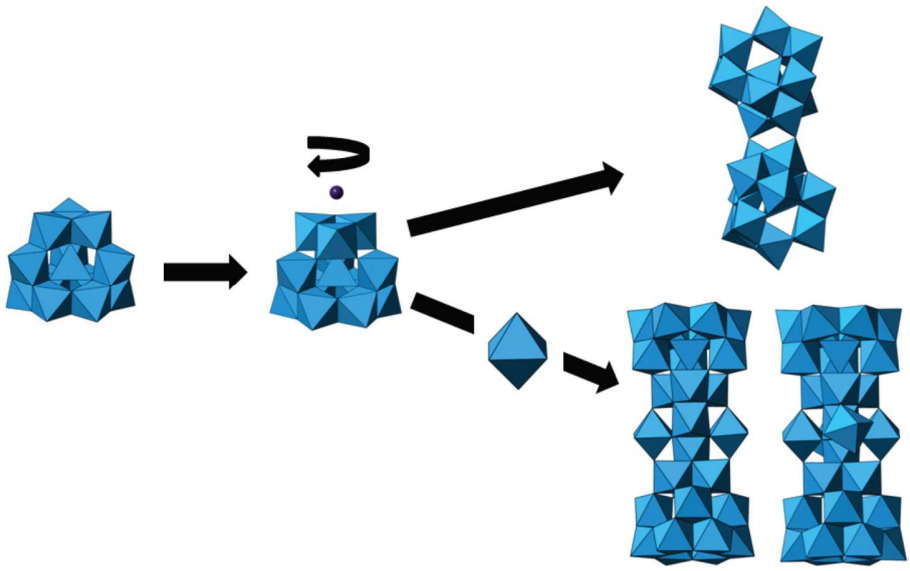

Figure 7. Formation mechanism of the large polymeric species Al_{26}, Al_{30}, and Al_{32}S (Reproduced with permission from Abeysinghe et al, 2012).

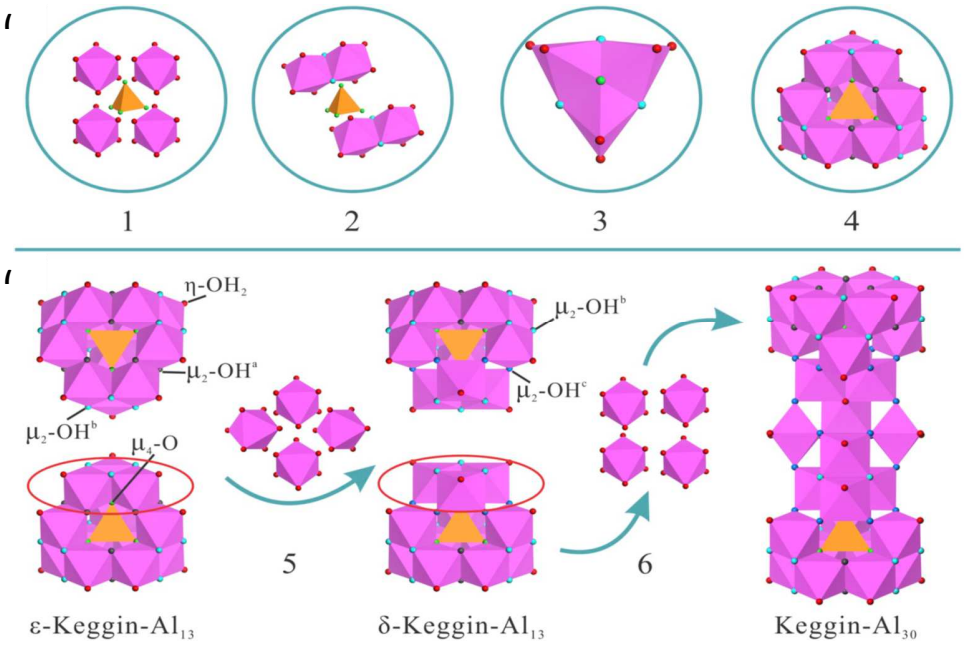

Figure 8. Formation process of the polycations Keggin-Al_{13} **(a)** and Keggin-Al_{30} **(b)** (Reproduced with permission from Wen et al, 2019a).

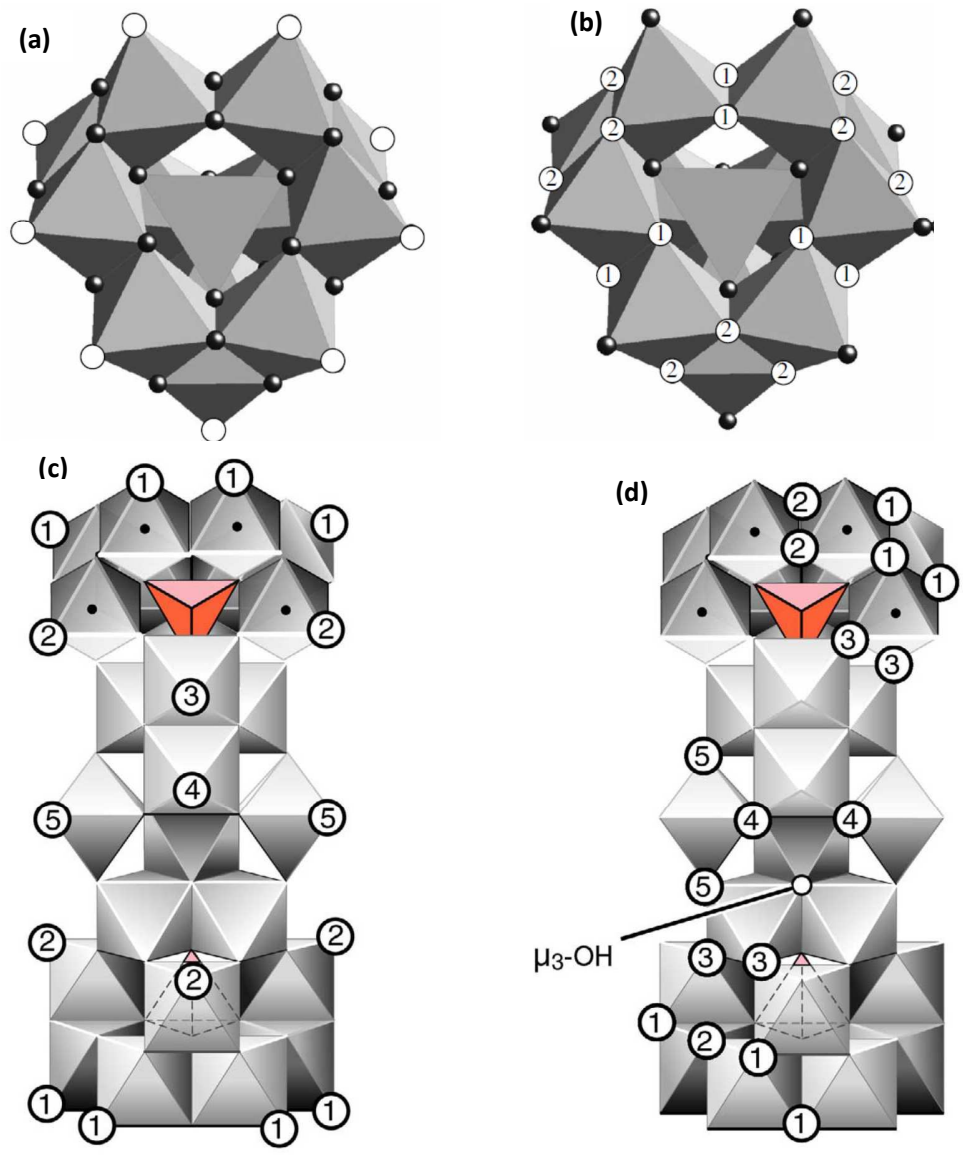

Figure 9. Surface functional groups: **(a, c)** Bound water molecules (η-H_2O) in Al_{13} and Al_{30}, respectively; **(b, d)** bridging hydroxide ions in Al_{13} and Al_{30} respectively (Reproduced with permission from Rustad, 2005).

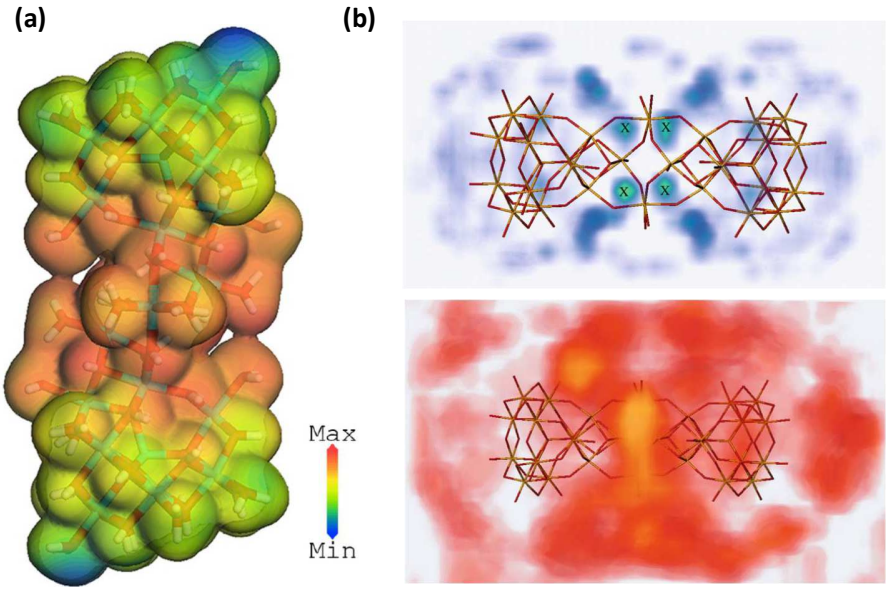

Figure 10. (a) Surface charge density of Al_{30}^{16+} (Reproduced with permission from Abeysinghe et al, 2013). **(b)** Outer-sphere water molecule (top) and anion (bottom) distribution around an Al_{30} molecule in skeletal form (Reproduced with permission from Casey et al., 2005).

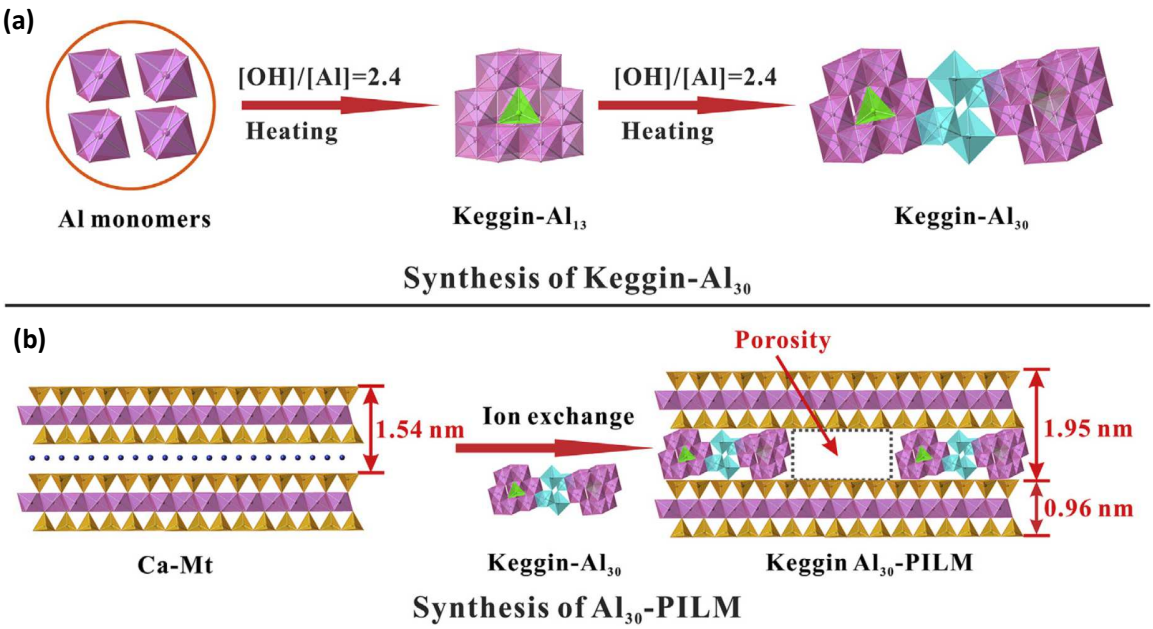

Figure 11. Representation of the synthesis of Al_{30} **(a)** and Al_{30}-PILC montmorillonite **(b)** (Reproduced with permission from Zhu et al., 2017).

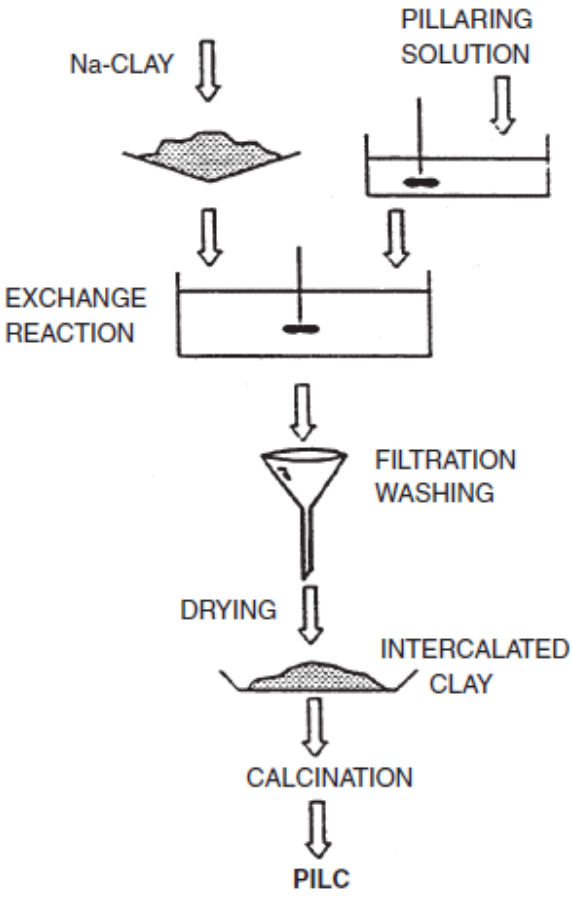

Figure 12. Pillared Interlayered Clays: general preparation procedure.

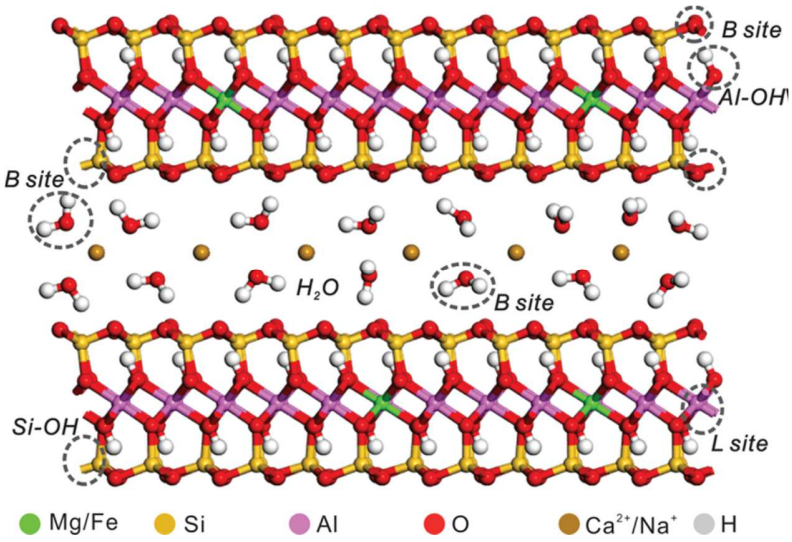

Figure 13. Possible acid sites in the montmorillonite (Reproduced with permission from Wen et al, 2019b).

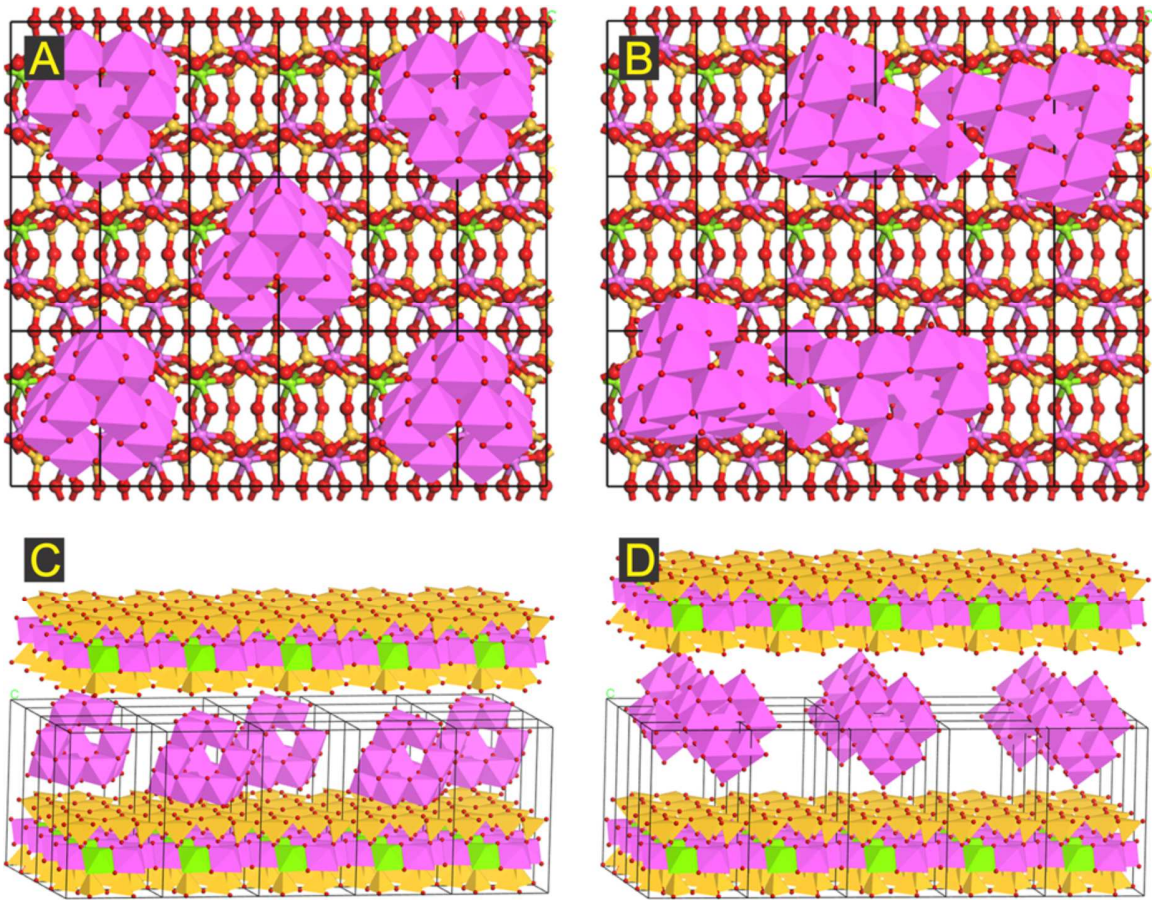

Figure 14. Al-polycation arrangement models in montmorillonite. Top view of Keggin polycations Al_{13} **(A)** and Al_{30} **(B)**, and three-dimensional view of Keggin polycations Al_{13} **(C)** and Al_{30} **(D)** (Reproduced with permission from Wen et al, 2019b).